SMHI RO
No.19, November 1994

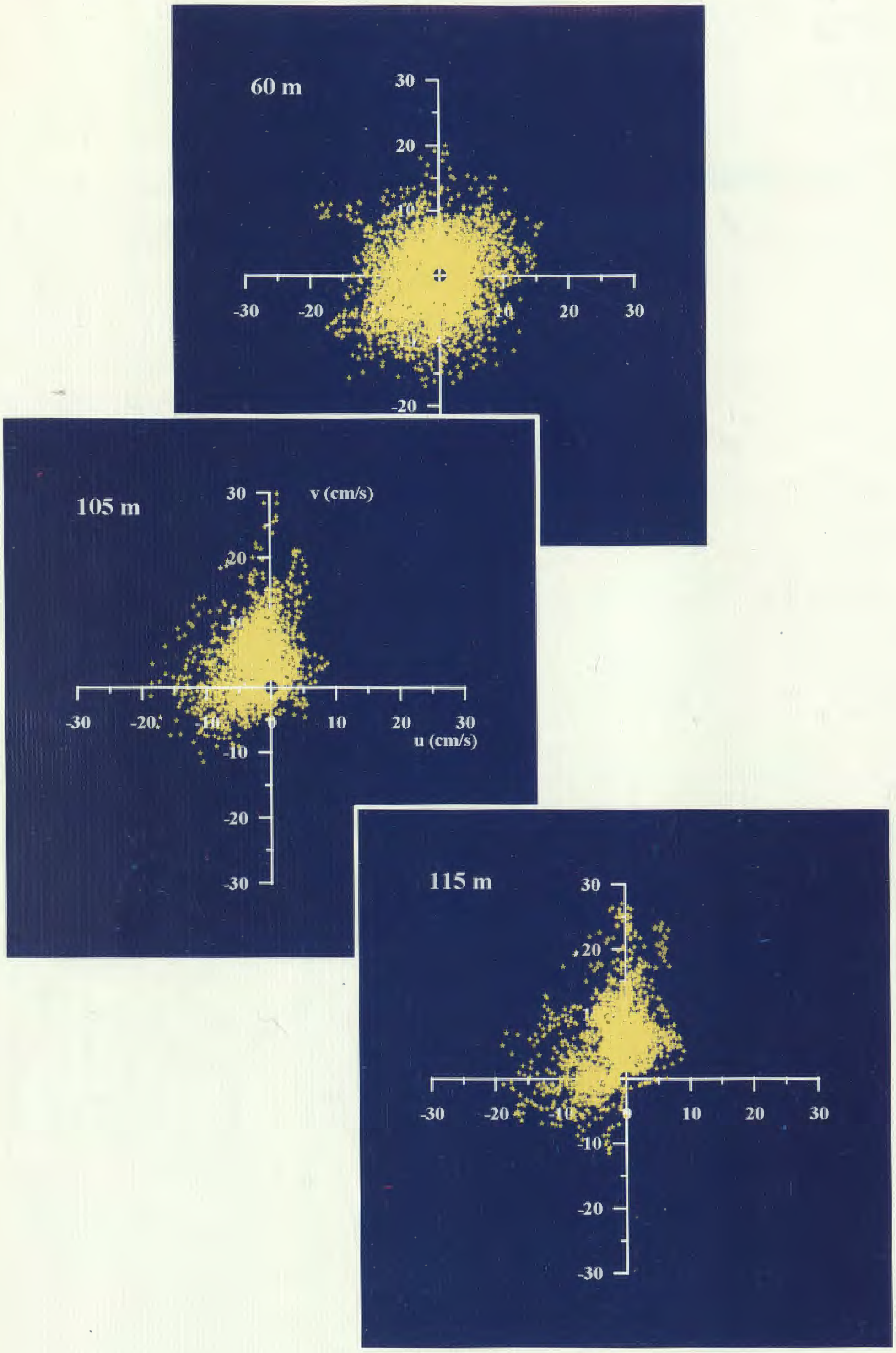

Currents in the Gulf of Bothnia During the Field Year of 1991

Eleonor Marmefelt

SMHI REPORTS OCEANOGRAPHY No.19, November 1994

Currents in the Gulf of Bothnia During the Field Year of 1991

Eleonor Marmefelt

Issuing Agency	Report number
Swedish Meteorological and Hydrological Inst. S-601 76 Norrköping Sweden	RO 19
	Report date 1994-11-07

Author (s)

Eleonor Marmefelt

Title (and Subtitle)

Currents in the Gulf of Bothnia
During the Field Year of 1991

Abstract

The Eularian experiment during the Gulf of Bothnia Field Year 1991 involved two dynamical experiments, the Open Sea Experiment and the Coastal Transect Experiment (Figure 1). The Open Sea Experiment covered one annual cycle while the Coastal Transect Experiment focused on a summer situation. One of the most striking observations made was the high velocities found near the bottom at all stations during the Open Sea Experiment.

Cont. on next page.

Key words

Coastal currents, deep water currents, resuspension

Supplementary notes	Number of pages	Language
	46	English

ISSN and title

ISSN 0283-1112

Report available from:

SMHI
S-601 76 Norrköping
Sweden

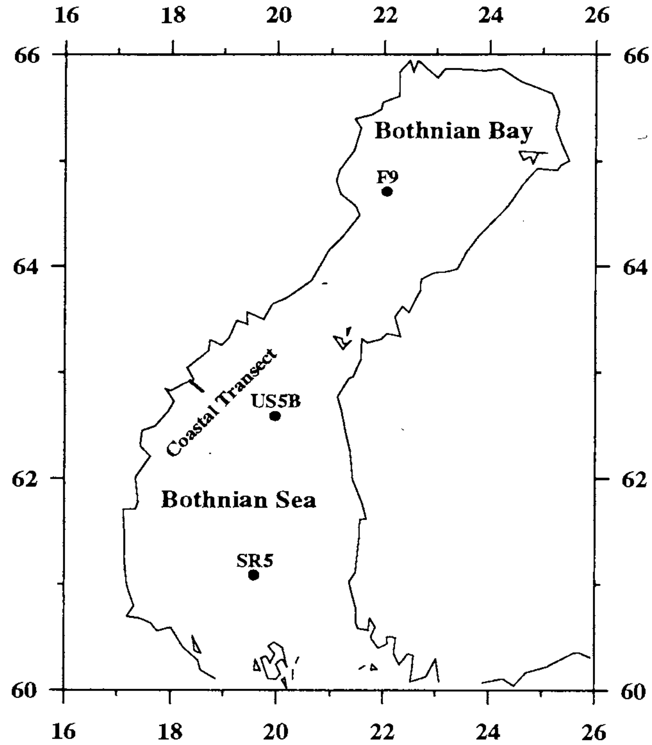

Figure 1. Location of the stations in the Open Sea Experiment (SR5, US5B and F9) and the Swedish Coastal Transect Experiment during the Gulf of Bothnia Field Year. The Open Sea Experiment was carried out from November 1990 until November 1991 and the Coastal Transect Experiment during one and a half month, starting on the 1st June 1991.

The Open Sea Experiment was carried out in the water body below the permanent pycnocline (i. e. below 60 m depth) and focused besides the deep water dynamics on the bottom currents impact on the sea floor. The strong currents observed near the bottom were occasionally able to resuspend loose material in the uppermost layer of the sediments. The currents have, especially in the Bothnian Sea, strong rotational response characteristics.

The coastal transect experiment was carried out in the wind induced surface layer. Data from this experiment show that the dynamical coastal zone of approximately 5 km width was present in the area. The velocity within the coastal zone increases towards the coast. The coastal currents mainly follow the coast southwards, probably caused by the large fresh water surplus in combination with bathymetric effects near the coast. The wind forcing of the coastal current is of minor importance. It requires days with relatively strong southerly winds before the main direction of the costal current turns northwards.

1. Introduction

The hydrographical conditions in the Gulf of Bothnia are quite unique with its brackish water and weak vertical stratification. The low salinity in the area is explained by large river runoff in the area but also by a shallow connection to the rest of the Baltic compared to the pycnocline depth in the Baltic Proper. The entrance area to the Gulf effectively prevents the more saline water in the deeper parts of the Baltic Proper to enter the Gulf. The river runoff itself causes together with the general circulation in the area a decrease in salinity northwards. The salinity surplus to the Gulf originates from the surface layer in the Baltic Proper. On its way into the Gulf the deep water becomes more diluted by freshwater from the rivers. The saline water that enters the Gulf moves along the Finnish coast and continues further into the Gulf in a counter clockwise path. The dilution by freshwater and entrainment of old, cold winter water from below contribute to the gradient of salinity as well as the gradient of temperature between the Finnish and the Swedish side of the Gulf.

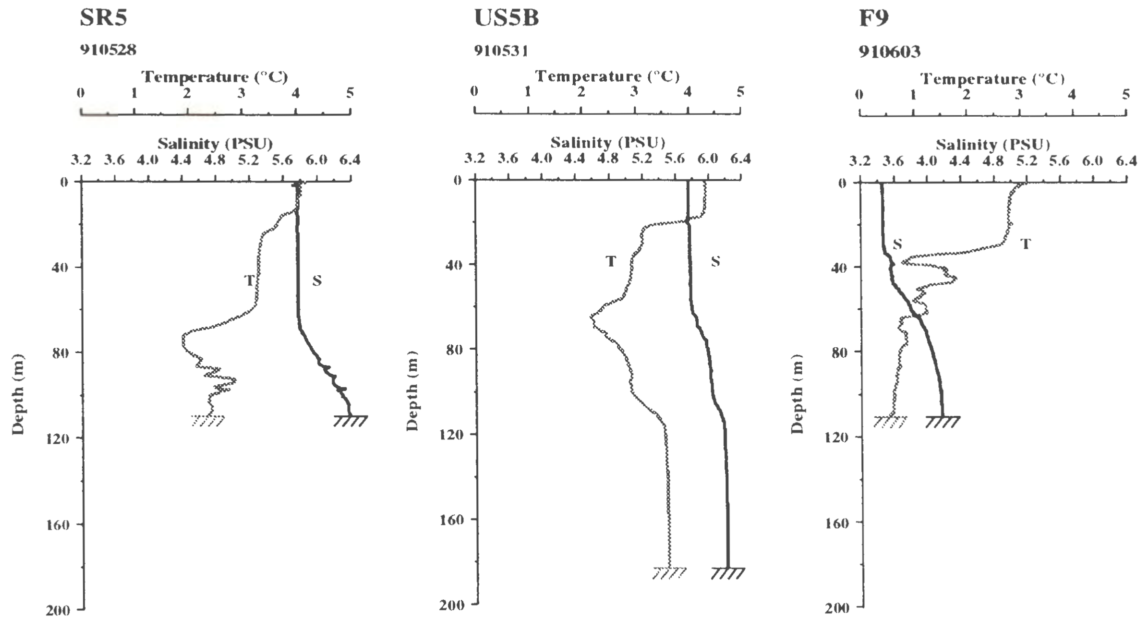

Figure 2. Vertical stratification of salinity and temperature from the three open sea stations. Although the difference of surface and bottom salinity is of order 1 PSU, the mixed layer depth can be discerned at 50 - 70 m depth. The weak halocline is actually able to effectively separate the surface water from the deep water and prevent complete turnovers within the entire water column. Data are taken from one of the hydrographic expeditions with R/V Argos during the Gulf of Bothnia Field Year.

Although the stratification in the Gulf seams weak (Figure 2) the well-mixed surface layer is efficiently separated from the deep water by the halocline. Thermal induced turnovers in the entire water column are rare processes within the area (Marmefelt and Omstedt, 1993a). They do occur, but they do not include the whole water column all the way to the bottom. Not even in the Bothnian Bay (where the difference between the surface salinity and the bottom salinity is approximately 1 PSU) there are any indications of total turnovers. However, one should keep in mind that, as the Bothnian Bay is completely covered with ice every winter, that limits the observations during winter time.

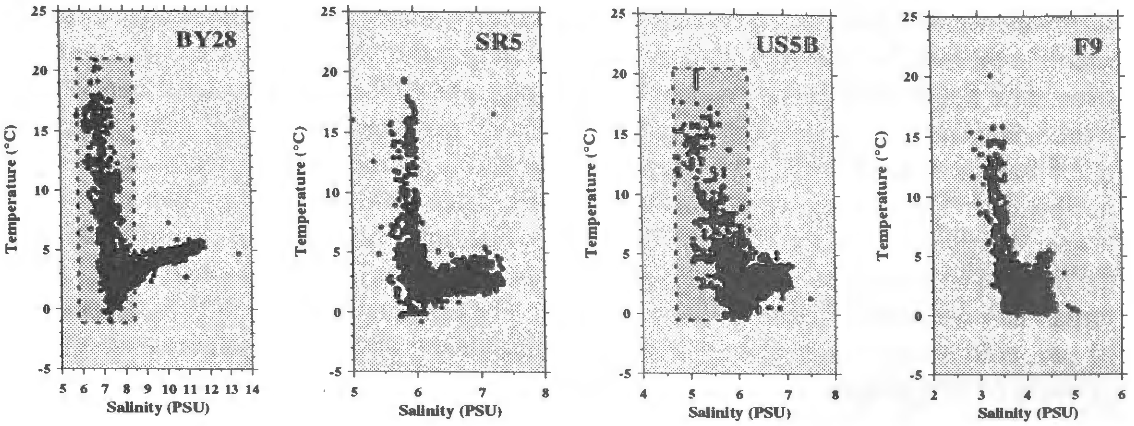

Figure 3. TS - diagram from the northern part of the Baltic Proper (BY28), the southern part of the Bothnian Sea (SR5), the northern part of the Bothnian Sea (US5B) and the southern part of the Bothnian Bay (F9). The marked area in the BY28 and the US5B diagrams roughly indicate the water above the sill depth of the entrance to the Bothnian Sea and the Bothnian Bay, respectively. Data are taken from the ICES data base covering the period from 1970 - 1990.

The deep water is renewed through major inflows of dense water (dense compared to the vertical stratification in the Gulf) originating from the Baltic Proper. As the sill depth to the Gulf of Bothnia is of the same order as the thickness of the surface layer in the Baltic Proper, the water entering the Gulf from the Baltic Proper originates from its surface layer. The deep water in the Baltic Proper is efficiently prevented from continuing further north by the sill. The Baltic Proper surface water has a low annual variation of salinity (Figure 3), the renewal of the deep water therefore takes place during the winter when the low sea surface temperature contributes to a high density of the incoming water. Dynamically the Gulf of Bothnia is therefore regarded as an estuary.

In an estuary like the Gulf of Bothnia, the area can be divided into three dynamically different zones; the open sea, the coastal zone and the straits. There are two straits in the Gulf. One of them, the Southern Quark, connects the Gulf to the Baltic Proper. The other one, called the Northern Quark, is situated within the Gulf and connects the Bothnian Sea to the Bothnian Bay. The Gulf of Bothnia Field Year, however, focuses on the coastal zone and the open sea.

2. The Coastal Zone

The coastal zone in the Gulf is exposed to a large extent of hazardous outlets, see e.g. Monitor 1988. Direct outlets and also the numerous river runoffs in the area (Bergström and Carlsson, 1993) contribute to the exposure of the coastal zone. The dynamics of the water transport in the coastal zone and its exchange processes with its environment are vital for the impact on the area.

The Coastal Transect Experiment was carried out near Högbonden in the northern part of the Bothnian Sea starting on the 1st June, 1991. Four Sensor data current meters were placed perpendicular to the local bathymetric contours at 12 m depth. The transect reached 8 km off the coast. The second mooring station off the coast also included a thermistor chain between 13 and 63 m depth, with the thermistors placed every 5th m. The moorings were carried out every 32nd minute. The duration of the transport experiment was limited by the storing capacity of the Sensor data meters and ended on the 17th July. The thermistors were active until the 17th September; see also Marmefelt and Omstedt (1993b).

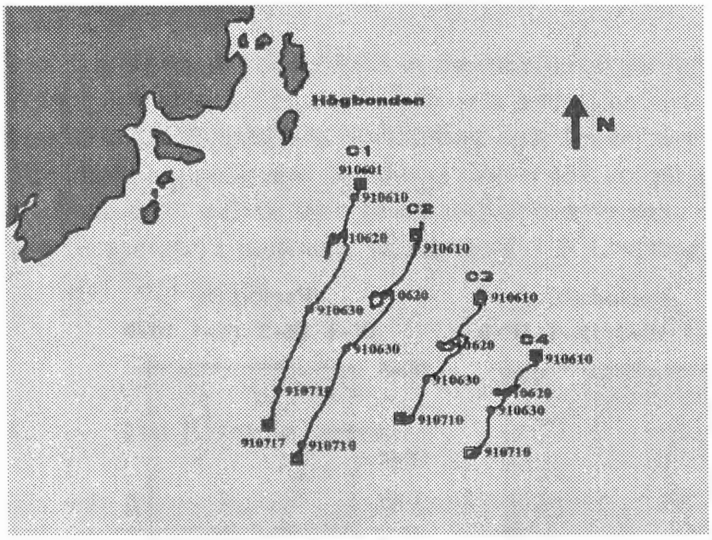

Figure 4. Progressive vector diagram from the Swedish Coastal Transect Experiment. The water transport within the coastal boundary zone is mainly following the coast southwards. Strong southerly winds turn the direction of the water transports northwards, but weak, fluctuating winds are not able to affect the main southward path.

The coastal zone experiment was carried out well within the wind-induced surface layer. Observed currents were influenced by the wind, but, as expected, limited by the vicinity of the coast. The current pattern corresponds to a typical coastal boundary layer pattern, with the currents following the coast, and the speed decreases with the increasing distance to the coast (Figure 4 and Appendix B).

As long as the winds were weak, the surface water mainly followed the coast southwards despite the wind direction. It requires fairly strong northerly winds to change the direction of the transports in the coastal zone. The transports within the surface layer are probably forced by the freshwater surplus, mainly from the rivers. The large river runoff in the area contributes to sustain the main circulation in the surface layer.

Although the average circulation is anticlockwise, the transport in the surface layer is highly transient. Energy spectra (Figure 5) are of great help for studying the transient nature of the transports. The main part of the transport during the Coastal Transect Experiment varied with low frequency compared to the measuring period of 45 days, coupled to the response of the changes in the weather conditions within the surface layer.

The high frequency changes in the wind do not affect the water transport in the coastal zone to the same extent. The coast and the local bathymetry affect the low frequency motions so that their main energy content is found in the velocity component along the coast or the local bathymetry (Appendix C1 - C4). The difference in energy content of the velocity components are more outspoken at the stations near the coast, where the coast as well as the local bathymetry are obvious, the further distance to the shore the smaller differences between the components (along and across the shore respectively) of the slow variations.

The total energy content reduces with the distance off the coast, an effect of the waves trapped by the coast due to the earth's rotation (Omstedt et. al., 1993).

Except for the high energy content of low frequency motions only one energy peak in the energy spectra is significant at all four stations, namely the peak at the inertial period.

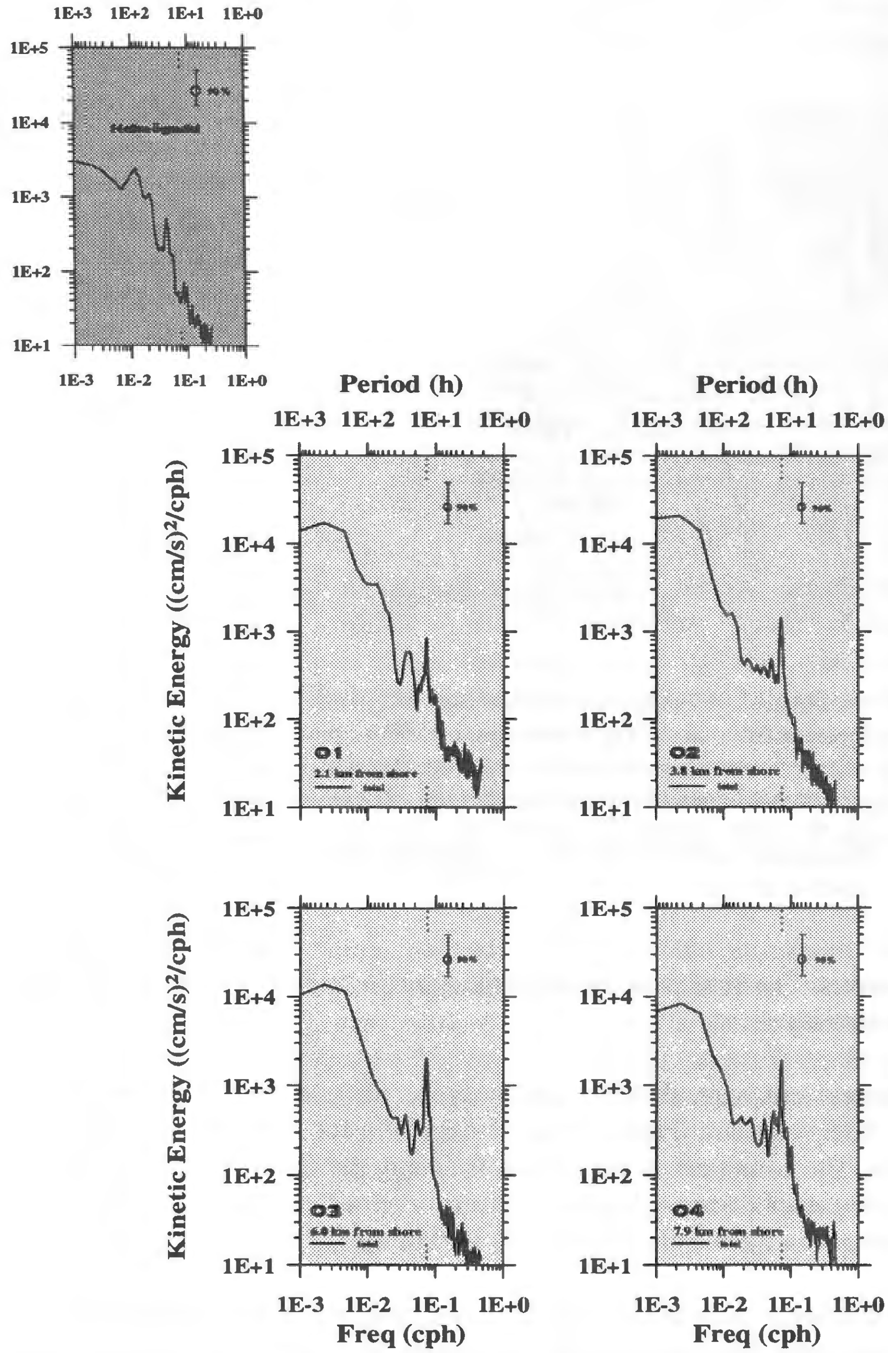

Figure 5. Energy spectra from weather station Holmögadd, stations C1, C2, C3 and C4 (2.1 km , 3.8 km, 6.0 km and 7.9 km off the shore respectively). Most of the energy content is associated with low frequency oscillations. The energy content is decreasing with the increasing distance off the coast. Inertial currents (period of 13.4 hours) are found at all stations during the Coastal Transect Experiment. At station C1 (and Holmögadd station) there is also one peak with a period of 24 hour representing the sea breeze.

Inertial currents are forced by the earth's rotation and have a period of 13.4 hours at the latitude of the coastal transect. The inertial currents are typical open sea phenomena. The vicinity of land prevents the clockwise circulation that the earth's rotation sets up. In an undisturbed area, the radius of the clockwise circulation (r) is determined from the velocity (v) and the earth rotation ($f = 1.25 \cdot 10^{-4}$) as $r \sim v/f$.The inertial currents are highly affected by the vicinity of the coast at least twice the radius off the coast. The average radius was of order 1 km during the experiment. The energy content at the inertial period is also found lower near the coast. Well outside the coastal boundary zone the energy content at the inertial period is not dependent of the distance to the coast (stations C3 and C4).

Sea breeze can be developed in the mornings during warm days when the sea surface temperature is low. The sea breeze only affects an area very close to the coast. An energy peak at a 24 hour period is therefore only found at station C1 in the energy spectra. A corresponding peak at a 24 hour period is also found in the wind spectra. The summer of 1991 was cold, with an average sea surface temperature 1 - 2°C below normal during June. The temperature increased in July to 1 - 2°C above normal at the end of the Coastal Transect Experiment.

3. The Open Sea Area

Not only the coastal zone in the Gulf is affected by the large amount of polluted outlets in the area. The open sea area will also be affected indirectly through water exchanged between the coastal zone and the open sea and by inflows from the Baltic Sea. The water exchange taking place between the coastal zone and the open sea can carry pollutants far away from the source. The effects on the open sea are in the end a consequence of the dynamics in the area. In some areas the currents near the bottom will transport the pollutants further away, but in other areas with low currents the pollutants are able to settle and the storage of hazardous outlets can be immense.

The Open Sea Experiment was carried out at three stations, located in the southern part of the Bothnian Bay (station F9), in the northern part (station US5B) and in the southern part (station SR5, at which the measurements were carried out by the FIMR) of the Bothnian Sea. The experiment focused on deep water dynamics. Three Aanderaa current meters where placed at each station at 60 m depth, and at 5 m and 15 m above the sea floor respectively. The moorings were carried out every hour during the entire Field Year, starting in the beginning of November 1990, except when the capacity of the technical equipment was exceeded. For further details about the experiment, see Marmefelt and Omstedt (1993b).

The three stations represent three dynamically different areas. The SR5 is situated near the entrance to the Gulf, the US5B in the inner part of the Bothnian Sea basin and the F9 near the entrance to the Bothnian Bay. The entrance areas to the Bothnian Sea (i.e. the entire Gulf) and the Bothnian Bay are dynamically very different. The Southern Quark is relatively deep and narrow. The water is transported through a deep canyon when it passes through the entrance area on its way into the Bothnian Sea. In that way the incoming water does not get in contact with surrounding water to any larger extent and it can carry on into the Bothnian Sea rather unaffectedly. The Northern Quark (the connection between the

Bothnian Sea and the Bothnian Bay) is a shallow area where the bottom friction influences the transports and mixes the water down efficiently (Marmefelt and Omstedt, 1993a). In that way there will be a large interaction with surrounding water in the Northern Quark, and the incoming water becomes highly diluted with less dense water before entering the Bothnian Bay.

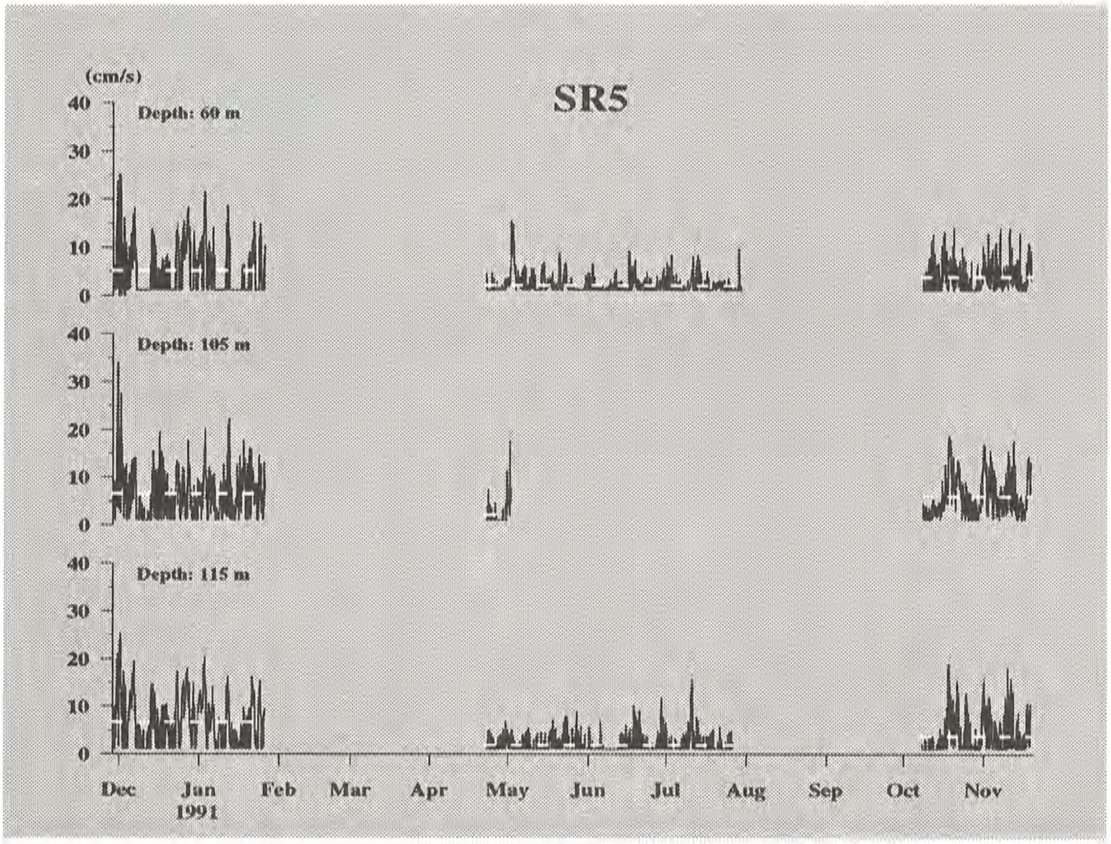

Figure 6. Current speed from the station SR5 during the Open Sea Experiment. The average speed for every period and observation depth is marked with a white dashed line. Corresponding speeds from the stations US5B and F9 are found in Appendix C5 - C6

The currents in the deep water are remarkably strong even 5 m above the sea floor. The average speed near the bottom varies from 2.1 cm/s to 6.7 cm/s during the observational periods (Figure 6 and Appendix C5 - C6). The highest average velocities are found at the SR5, i.e. near the entrance to the Gulf. It is also interesting that at the SR5 the average velocities are higher 15 m above the sea floor than at depths just above the permanent pycnocline (situated at 65 - 70 m depth). This pattern is not found at the other stations, where the average velocities decrease smoothly with increasing depths. The main water transports in the deep water follow the local bathymetric contour (Appendix C7 - C9), although their direction is fluctuating a great deal.

In the northern part of the Bothnian Sea (Appendix C10 - C11), the water just above the permanent pycnocline moves almost continually northwards. Water at this depth can continue further north towards the Northern Quark without any major difficulties. The water at greater depths, however, is trapped within the Bothnian Sea. The average velocities are low, and the main direction is determined by the local bathymetric conditions.

Near the entrance to the Bothnian Bay the main water transport in the deep is northwards into the basin (Figure 7 and Appendix C12). The water transport just above the permanent pycnocline varies more due to the wind influence, although it is mainly southwards to compensate the incoming dense water in the deep. On its way into the Bothnian Bay the inflowing water is not confronted with any major impediments, like more shallow areas. It probably follows the smoothly sloping bottom continuously in time once it has left the Northern Quark.

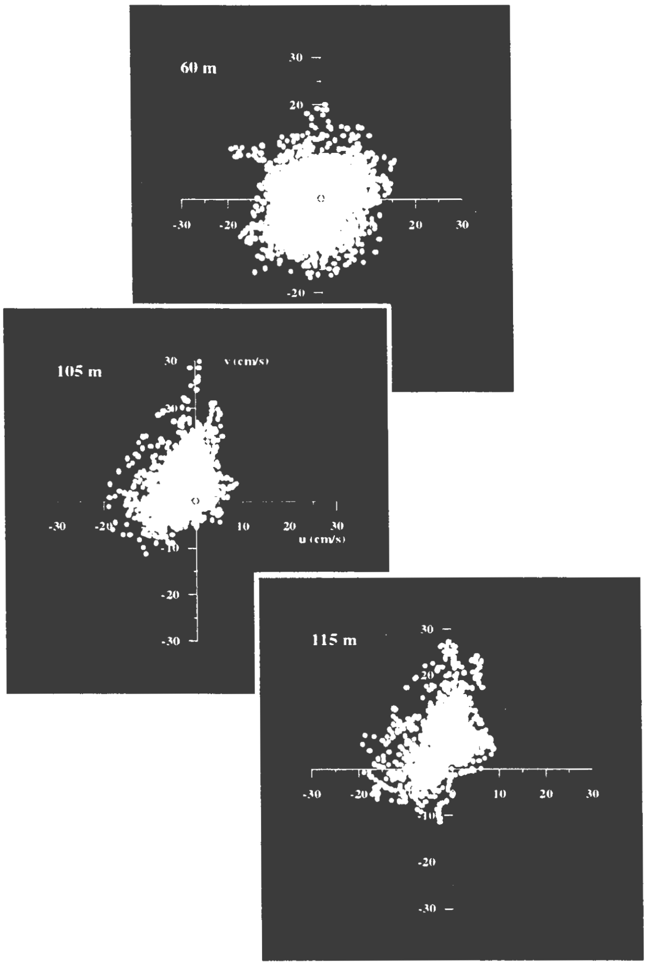

Figure 7. u-components vs v-components from the station F9 during the first observation period. The direction of the transports at 60 m depth are highly fluctuating, while they near the bottom tends to follow the local bathymetry. The velocities are occasionally extremely highnear the bottom.

The characteristics of the transports are, as we have seen, very transient even near the bottom. The characteristics of the deep water transports show very distinct similarities near the entrances (station SR5, Appendix C13 - C15, and F9, Appendix C16 - C18), where the inertial currents are present at all depth during all observational periods. In the southern part of the Bothnian Sea the inertial currents below the wind induced surface layer are generated by the horizontal water-level slope (Marmefelt and Omstedt, 1994). The similar pattern found in the Bothnian Bay supports the idea that the inertial currents are generated in the same way here. In the northern part of the Bothnian Sea (Appendix C19 - C21), where the transports are not directly influenced by the inflowing dynamics, the inertial currents are only found in the surface layer during the second observational period, i.e. during the summer and autumn. On the other hand, the peak at the inertial period is the only significant one during this period. Other interesting phenomena that can be distinguished from the data are e.g. transports with a period of 11 days (found in the surface layer during the second observational period), which is the theoretical period for the seiche of the Kattegat-Skagerrak-Baltic Sea system (Svansson, 1980).

The strong velocities being observed during the Gulf of Bothnia Field Year most certainly

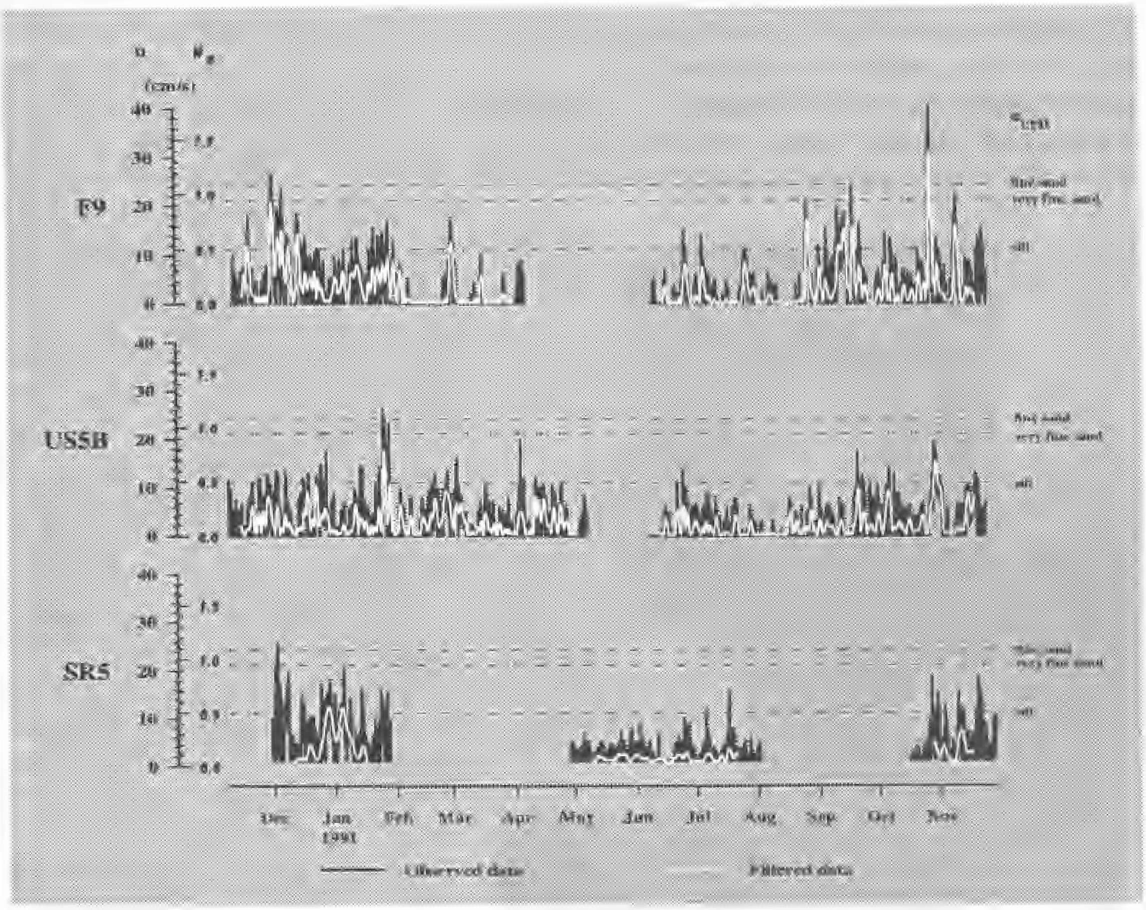

Figure 8. Currents observed 5 m above the sea floor at the stations F9, US5B and SR5 during the Open Sea Experiment. Critical velocities of resuspension for those depths are indicated for silt, very fine sand and fine sand. They are adjusted to the 5 m level by an ordinary logarithmic velocity profile. In addition the observed data have been filtered through a low pass filter with a 18 to 24 hour cut-off. The high frequency motions are mostly necessary to cause a resuspension in the area. It is very interesting to note how frequent those periods with high speeds are even so close to the bottom as 5 m, especially when taking into account that all three stations are placed in areas where the bottoms are classified as accumulation bottoms.

affect the sea floor itself. The average speed 5 m above the sea floor is between 1.0 and 2.4 cm/s (Appendix B), but speeds above 10 cm/s were quite frequent during the experiment (Figure 8). The strong currents set up a bottom boundary layer that is highly turbulent. The turbulent motion near the bottom can dislodge loose particles from the sea floor. Once suspended into the water the sediment particles are carried away with the water transport until they reach areas where the water transports are less intense and where they could settle again. Through cycles of resuspension, advection and finally resedimentation the particles can be carried away far from the coastal zone and their source before they finally settle again. The critical velocities for resuspension are based on the properties of the turbulence within the bottom boundary layer and on properties of the sediment grain itself (Dyer, 1986 and Appendix A). The bottom boundary layer is thin, of order 1 m, and moorings made 5 m above are not able to catch the dynamics within the bottom boundary layer. The roughness of the bottom itself decreases the motions almost completely by friction. The threshold velocities for different sizes of the particles have therefore been adjusted to the 5

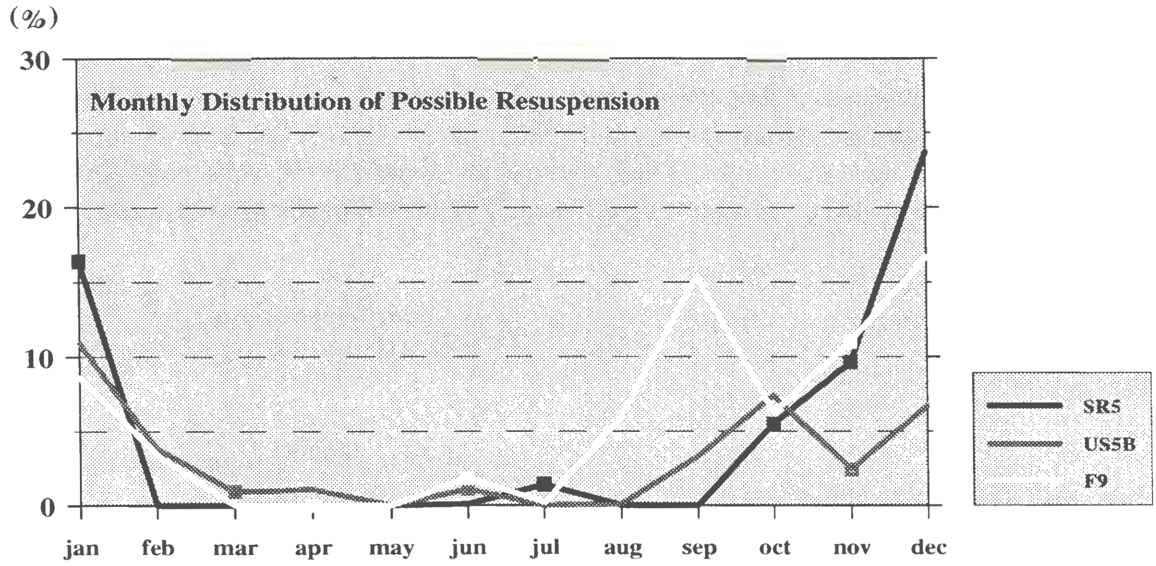

Figure 9. Monthly distribution of possible resuspension obtained from the simple assumption that the current velocities are associated to the resuspension through the size of the sediment grain. Months when the observations did not cover the entire month are marked with a square.

m level above the sea floor by an ordinary logarithmic velocity profile.

All three stations are placed in areas where the bottoms are classified as typical accumulation bottoms (Brydsten, 1993), where the currents near the bottom is supposed to be so low that resuspension is not possible. Nevertheless, the calculations show that the observed currents are strong enough to resuspend the settled materia, but also that it mostly requires high-frequency motion superimposed on the low-frequency transport for resuspension to occur. The possible resuspension is more intense and frequent during autumn and winter near the entrances (Figure 9), related to more vigorous water-level forcing. In the northern part of the Bothnian Sea the annual distribution of events with resuspension is not as apparent as near the entrances, although resuspension is also more common during January far away from the entrance areas. The classification where the bottoms in the area are thought to be accumulation bottoms is based on the assumption that the resuspension can be determined directly from the wind fetch and the wave energy in the area and does not account for the currents near the sea floor.

Summary

The observations made during the Gulf of Bothnia Field Year 1991 have shown the complex dynamics in the area. Measurements made near the sea floor in areas where the bottoms are classified as typical accumulation bottoms, show that velocities of 20 - 30 cm/s are common also in those areas. It implies that the resuspension process cannot be overlooked. To be able to determine the resuspension one has to take the near bottom boundary layer currents into account as well as the local fetch and wave energy in the area.

The average circulation within the surface layer during the Field Year confirms the circulation pattern presented by Palmén in 1930, although it has been found highly transient. The vicinity to the coast and the local bathymetry have large effects on the transports, but also horizontally extended phenomena as inertial oscillations are present in the coastal zone.

References

Bergström, S. and B. Carlsson (1993)
Hydrology of the Baltic Basin. Inflow of fresh water from rivers and land for the period of 1950 - 1990.
SMHI RH No 7.

Brydsten, L. (1993)
Characterization of transport bottoms in the Gulf of Bothnia - a model approach.
Aqua Fennica 23(2)

Dyer, K. R. (1986)
Sediment Movements
Chapt 4. In: Coastal and Estuarine Sediment Dynamics. John Wiley & Sons, pp 108 - 143

Marmefelt, E., and A. Omstedt (1993a)
Deep Water Properties in the Gulf of Bothnia
Cont. Shelf Res, Vol 13, No 2/3, pp 169 - 187

Marmefelt, E., and A. Omstedt (1993b)
Swedish Eularian Current Measurements
Chapt 2. In: The Gulf of Bothnia Field Year 1991. Physical Transport Experiments. Ed C. R. Murthy, B. Håkansson and P. Alenius. SMHI RO No 15.

Marmefelt, E. and A. Omstedt (1994)
On the Generation of Inertial Oscillation in a Semi Enclosed Basin
Geophysica (in press)

Monitor 1988
Östersjön och Västerhavet - livsmiljöer i förändring.
Statens Naturvårdsverk, Solna, Sverige

Omstedt, A., E. Marmefelt and R. Murthy (1993)
Some Flow Characteristics of the Costal Boundary Layer in the Bothnian Sea
Aqua Fennica 23, 1, pp 5 - 16

Palmén, E. (1930)
Untersuchungen über die Strömungen in den Finnland umgebenden Meeren
Soc. Scient. Fenn. Comm. Phys - Math. Vol 12

Svansson, A. (1980)
Exchange of Water and Salt in the Baltic and Adjacent Seas
Oceanologica Acta, vol 3, No 4, pp 431 - 440

Appendix A

Critical Conditions for Resuspension

The critical conditions for resuspension is based on turbulence characteristics of the oscillations near the bottom, which can be described by a grain Reynold number, based on the particle's diameter:

$$Re = \frac{Du_*}{\nu}, \tag{1}$$

where D is the particle diameter, u_* the friction velocity and ν the kinematic viscosity. The friction velocity is determined through a conventional drag law,

$$u_* = \sqrt{c_d}\, u \ ,$$

where the drag coefficient c_d is put equal to $2 \cdot 10^{-3}$. The velocity u is taken from the current meter at 5 m above the sea floor. The turbulent boundary flow can be regarded as smooth when the particle Reynold number is below 5.0 (Dyer, 1986), which is the case in this study. A threshold shear stress for resuspension within a smooth turbulent flow can be determined by (op. cit. White, 1970):

$$\left(u_{*crit}\right)^{\frac{5}{2}} = 0.06\, g\left[\frac{\rho_g - \rho_0}{\rho_0}\right]\nu^{\frac{1}{2}} D^{\frac{1}{2}}, \tag{2}$$

where ρ_g is the density of the sediment grain.

Swedish current measurements:

Station	Depth (m)	Period	u (cm/s)		v (cm/s)		Salinity (PSU)		Temperature (°C)	
			average	variance	average	variance	average	variance	average	variance
US5B	60	7/11-11/5	.41	11.85	3.67	16.88	5.77	.21	2.71	2.72
US5B	60	9/6-15/11	.25	23.04	2.43	29.44	5.75	.01	3.68	1.23
US5B	110	7/11-19/4	.27	20.72	1.67	15.00	6.13	.13	3.64	.16
US5B	110	2/6-15/11	1.18	8.89	1.35	9.18	6.10	.01	3.09	.07
US5B	120	7/11-3/5	.34	18.59	.55	7.06	6.00	.00	3.63	.10
US5B	120	2/6-15/11	.66	6.38	1.14	7.71	6.15	.01	3.14	.08
F9	60	9/11-8/5	-.55	15.50	-.17	15.99	3.43	.14	1.58	2.22
F9	60	3/6-16/11	-1.86	22.04	.19	21.40	3.61	.01	2.64	.48
F9	105	9/11-28/3	-1.16	7.50	1.88	14.67	4.02	.01	3.61	.39
F9	105	3/6-16/11	-.62	9.46	1.60	14.22	4.00	.00	1.91	.77
F9	115	9/11-3/4	-.61	7.00	2.25	19.32	3.98	.22	3.50	.65
F9	115	3/6-16/11	-.47	7.96	2.01	20.66	4.07	.00	2.00	1.10
C1	2.1*)	1/6-17/7	-8.31	115.96	-3.27	60.27	-	-	9.28	3.30
C2	3.8*)	1/6-17/7	-7.9	96.16	-4.29	73.28	-	-	8.29	1.76
C3	6.0*)	1/6-17/7	-4.21	70.40	-2.85	65.72	-	-	5.75	1.91
C4	7.9*)	1/6-17/7	-3.45	43.67	-2.39	54.29	-	-	9.37	4.65

*) Distance from shore (km)

Finnish current measurements:

Station	Depth (m)	Period	u (cm/s)		v (cm/s)		Salinity (PSU)		Temperature (°C)	
			average	variance	average	variance	average	variance	average	variance
SR5	60	28/11-26/1	-2.08	25.06	-.96	23.82	6.86	1.18	3.80	.15
SR5	60	23/4-30/7	-.26	2.85	-.35	4.45	5.99	.02	2.87	.27
SR5	60	9/10-20/11	.26	13.09	-.65	11.08	6.36	.09	4.86	2.61
SR5	103	28/11-26/1	-1.67	31.67	-1.32	29.08	6.35	.03	3.48	.15
SR5	103	23/4-2/5	-.99	1.82	1.12	5.20	6.66	.00	3.62	.00
SR5	103	9/10-20/11	-2.60	23.22	1.30	20.53	7.01	.35	5.46	.14
SR5	113	28/11-26/1	-2.84	28.21	-1.02	33.19	6.89	.00	3.92	.01
SR5	113	23/4-27/7	.11	3.00	-.12	3.25	6.59	.01	2.73	.25
SR5	113	9/10-20/11	-.36	14.02	1.24	12.09	7.27	.03	5.28	.22

Appendix C1

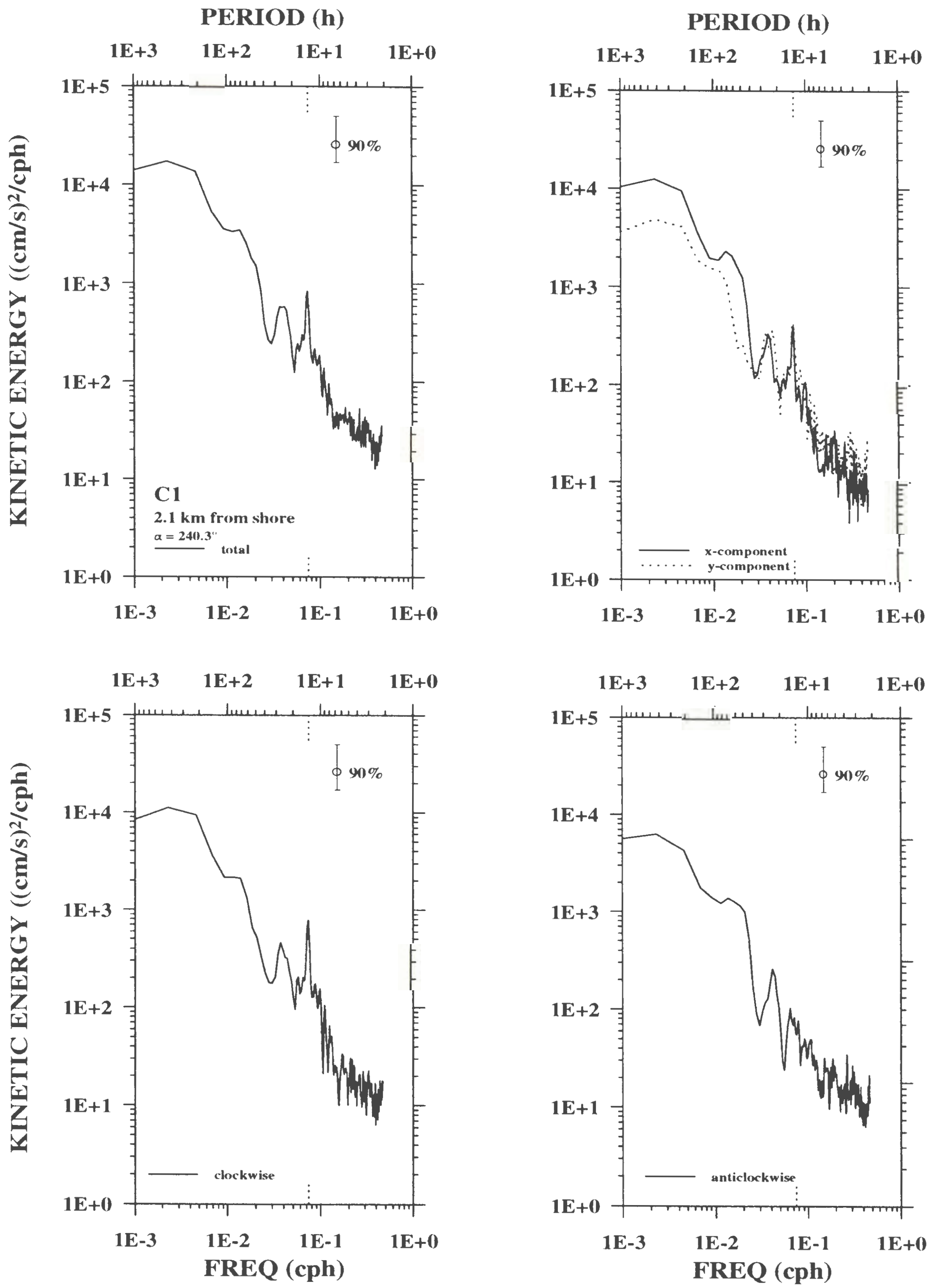

Appendix C1. Energy spectra from station C1 during the Coastal Transect Experiment.

Appendix C2

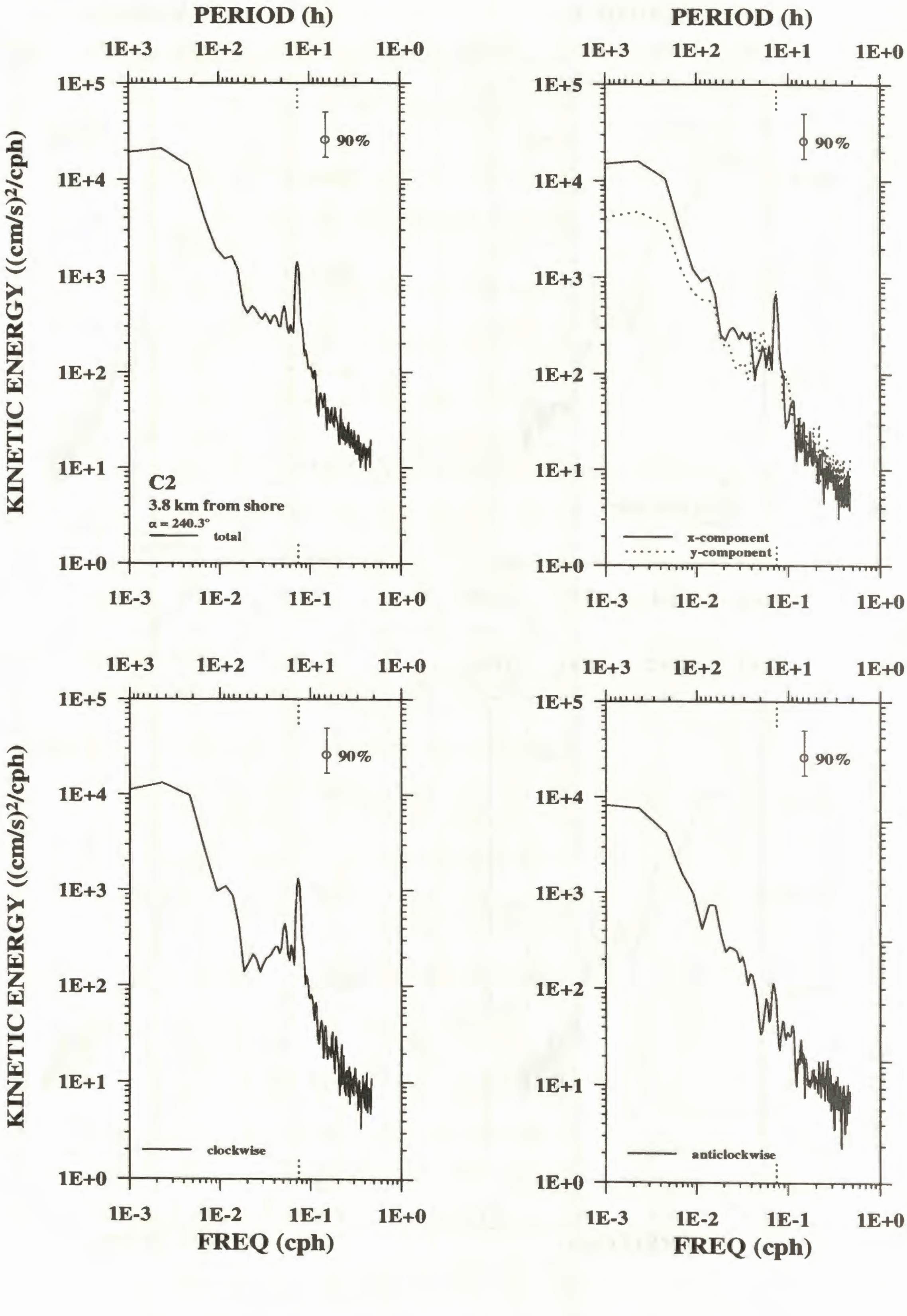

Appendix C2. Energy spectra from station C2 during the Coastal Transect Experiment.

Appendix C3

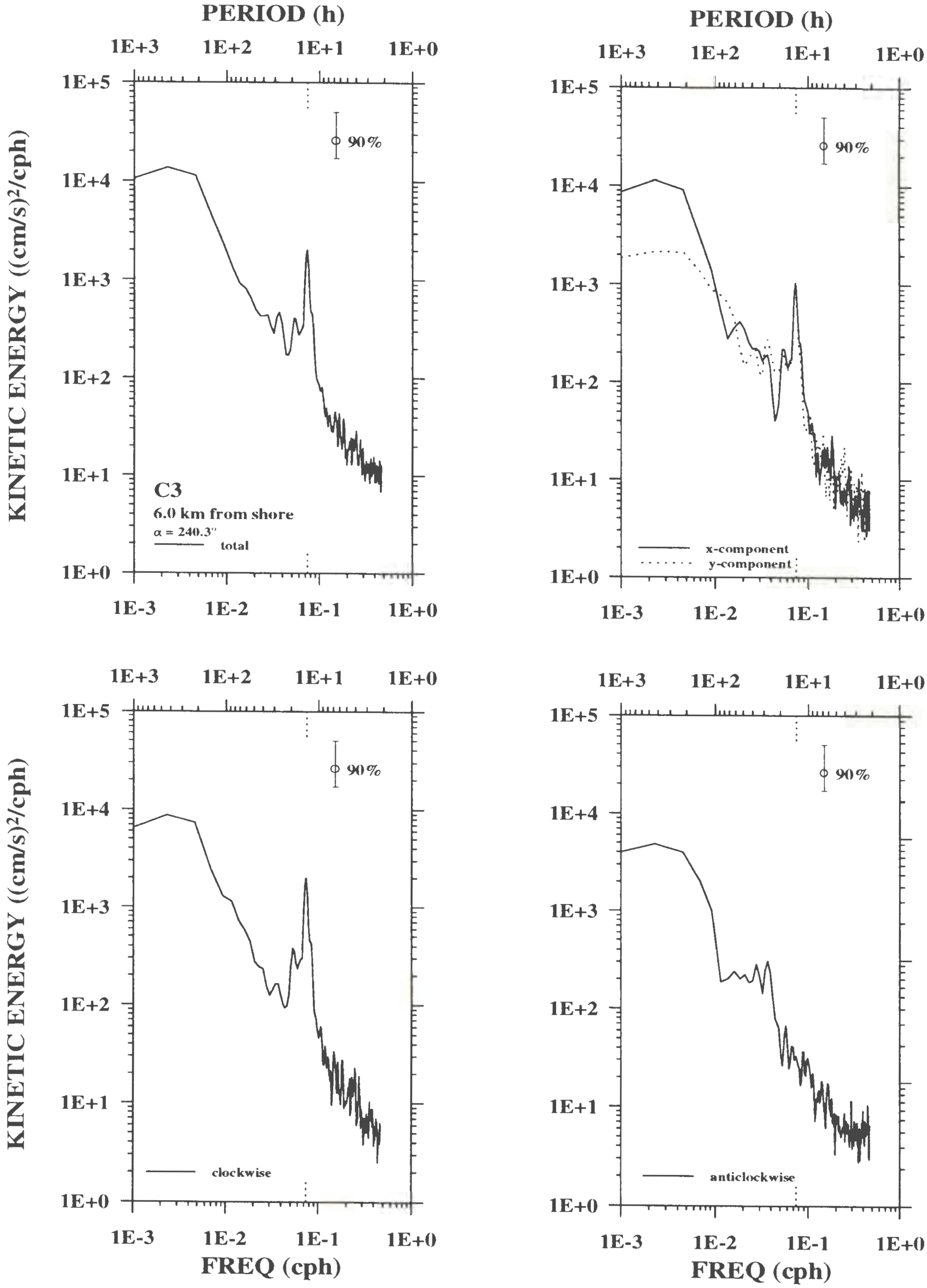

Appendix C3. Energy spectra from station C3 during the Coastal Transect Experiment.

Appendix C4

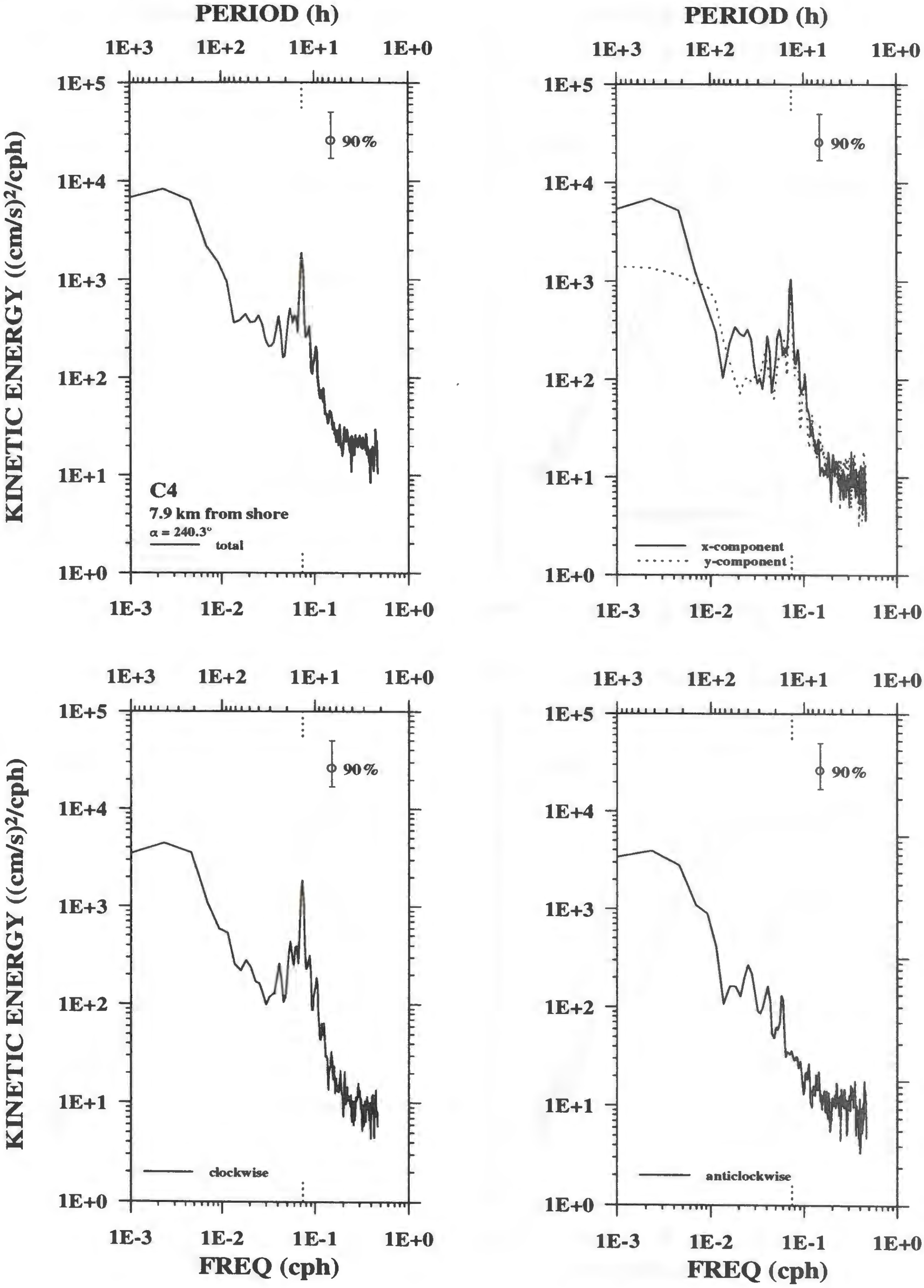

Appendix C4. Energy spectra from station C4 during the Coastal Transect Experiment.

Appendix C5

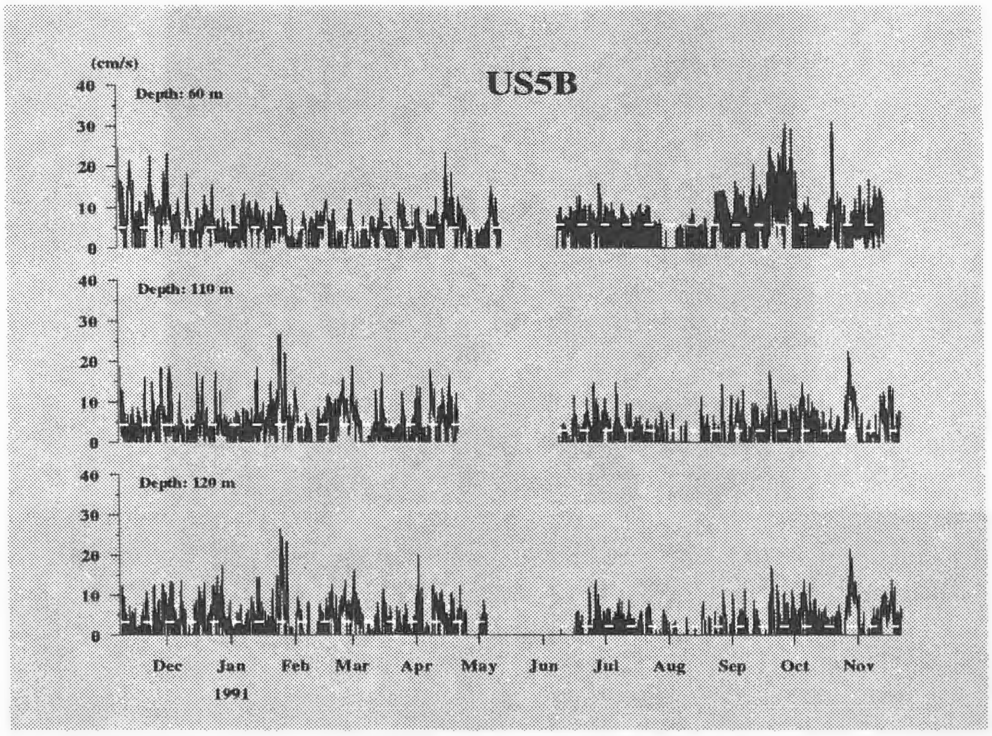

Appendix C6

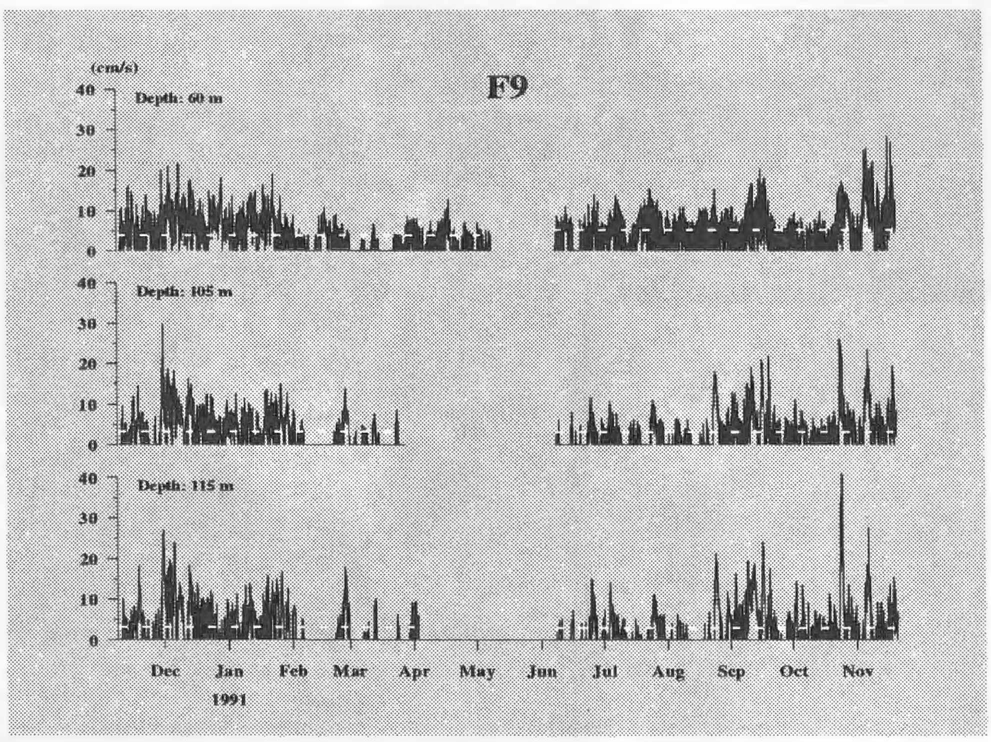

Appendix C5 and C6. Current speed from the stations US5B and F9 respectively. The dashed line mark the average speed for every period

Appendix C7

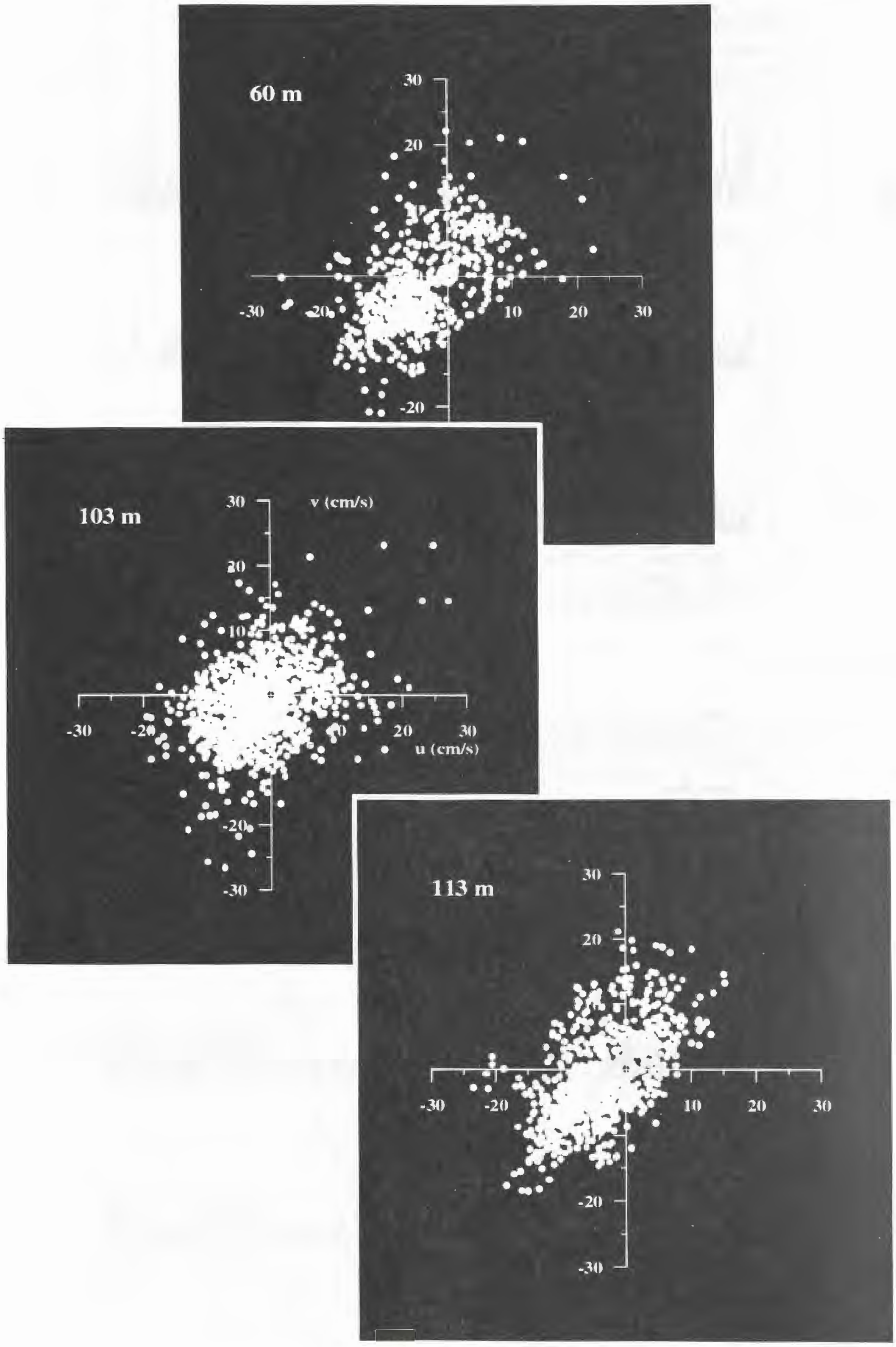

Appendix C7. u-components vs v-components from the station SR5 during the first period.

Appendix C8

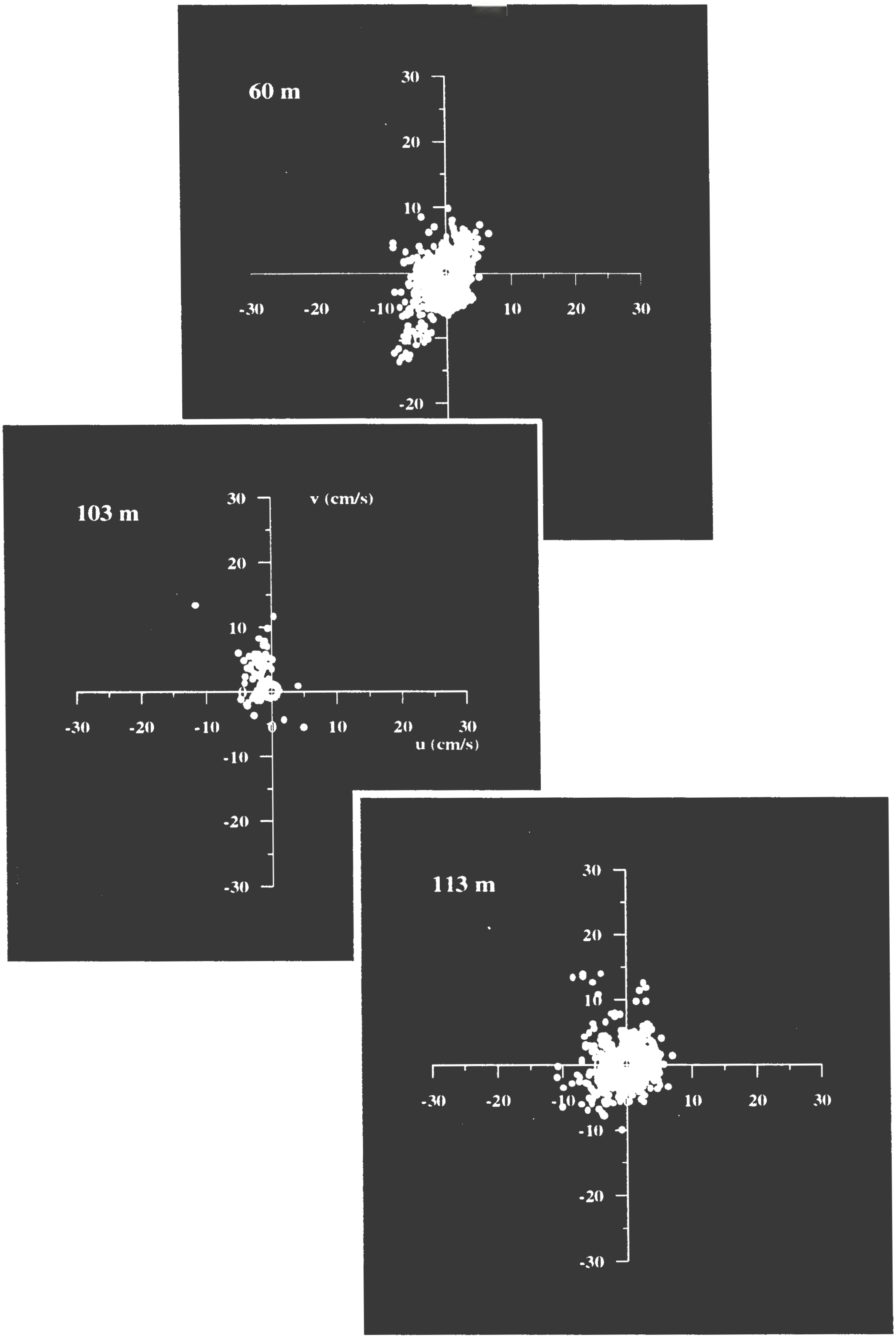

Appendix C8. u-components vs v-components from the station SR5 during the second period.

Appendix C9

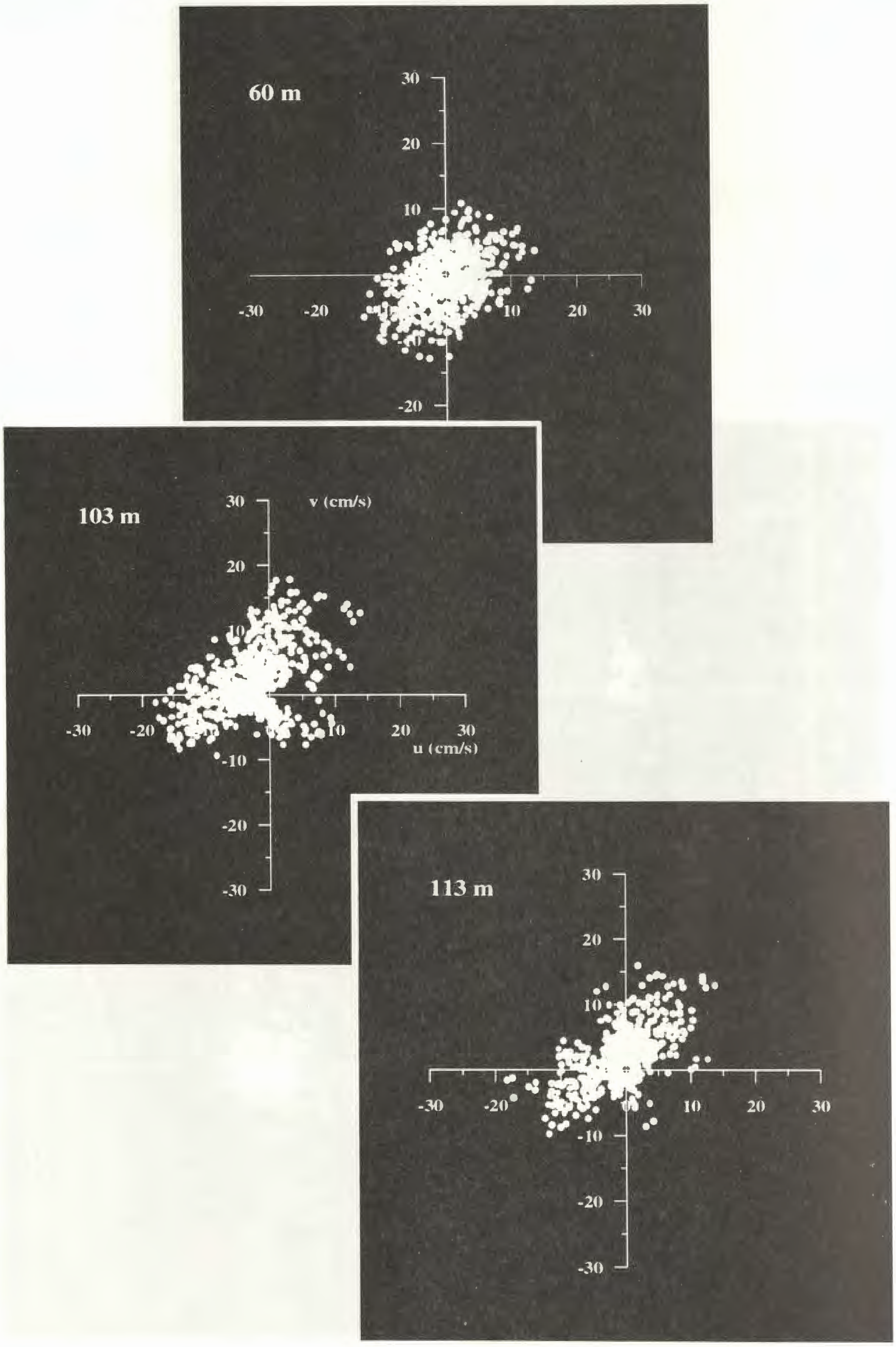

Appendix C9. u-components vs v-components from the station SR5 during the third period.

Appendix C10

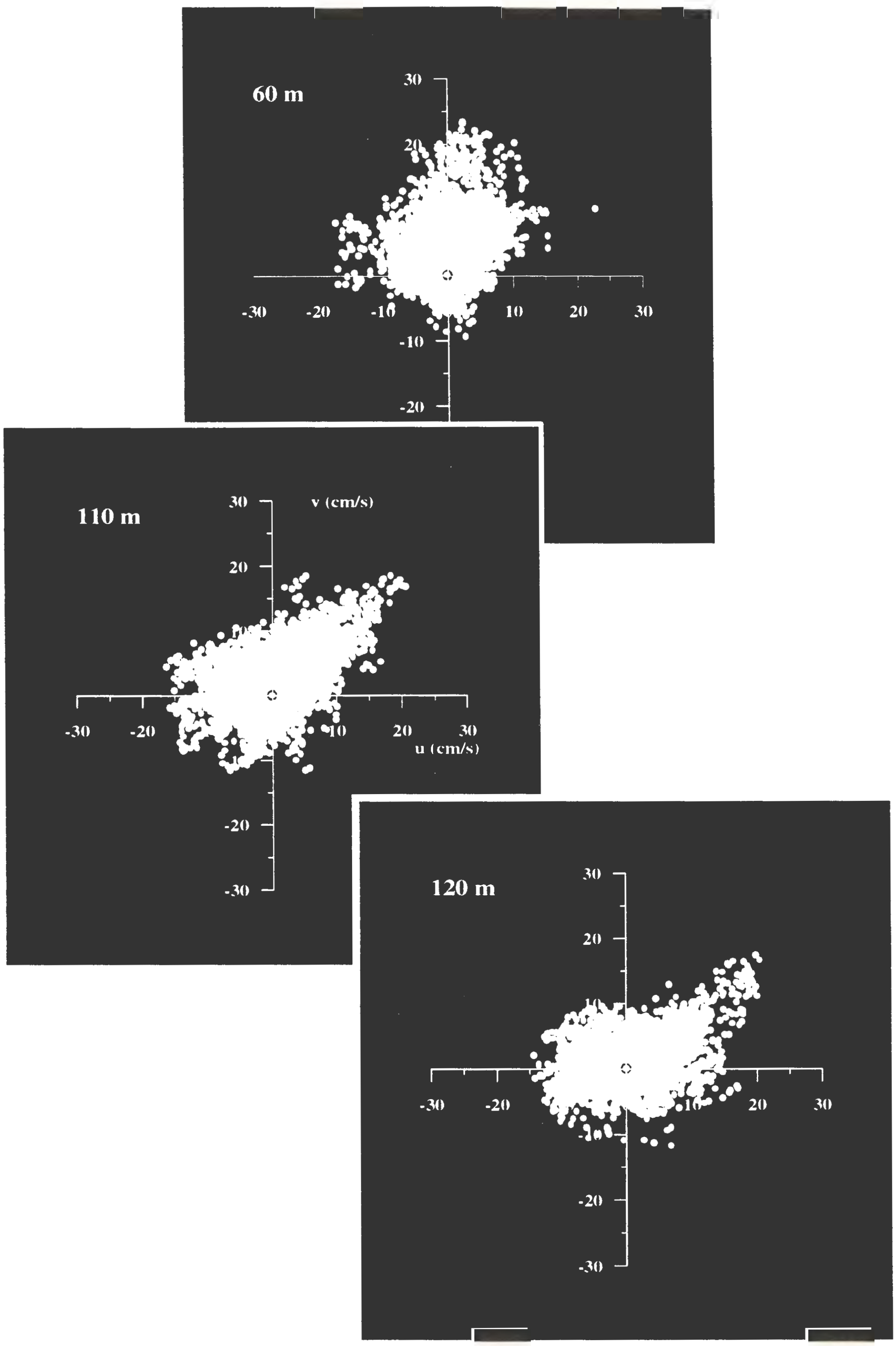

Appendix C10. u-components vs v-components from the station US5B during the first period.

Appendix C11

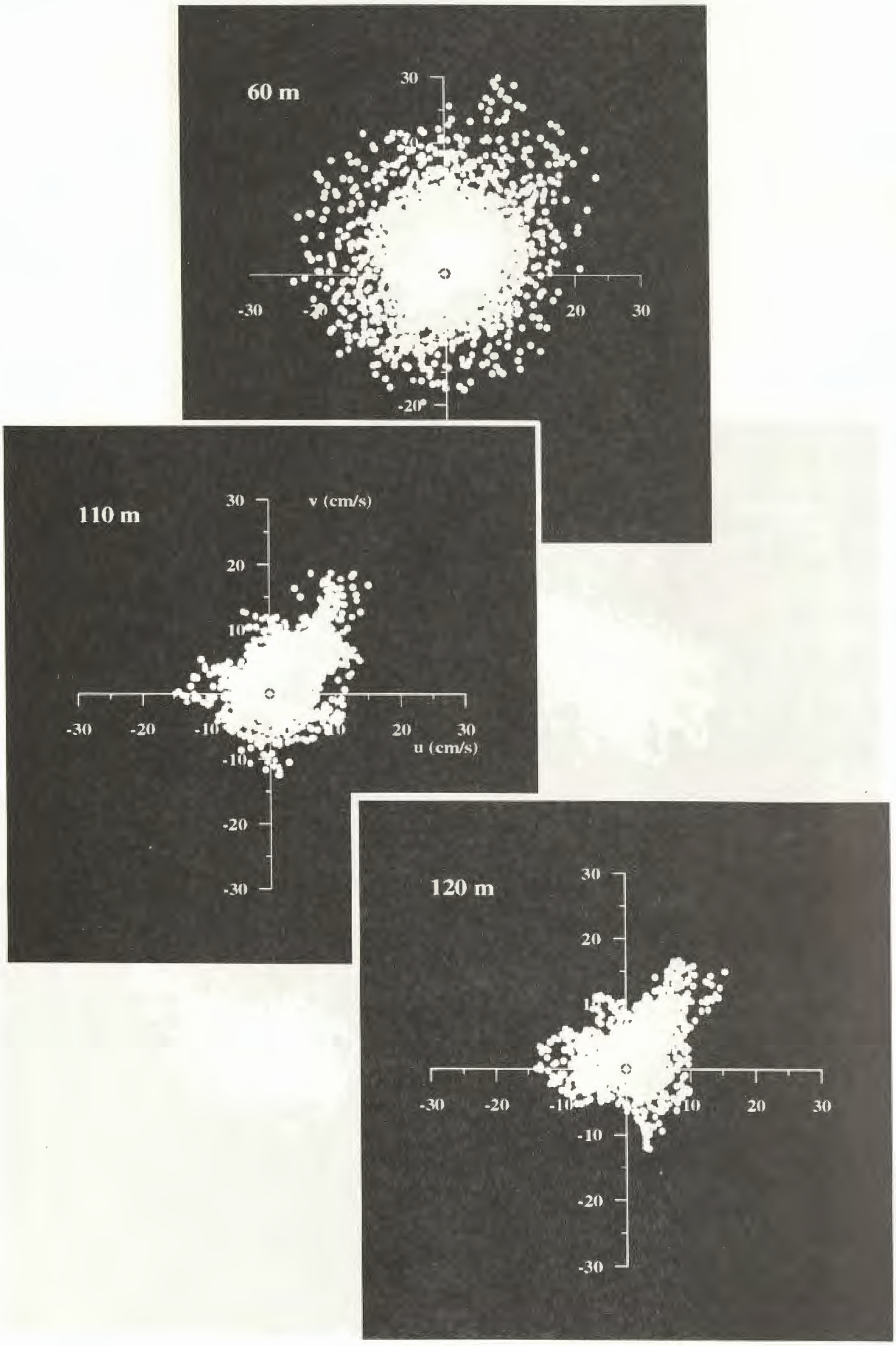

Appendix C11. u-components vs v-components from the station US5B during the second period.

Appendix C12

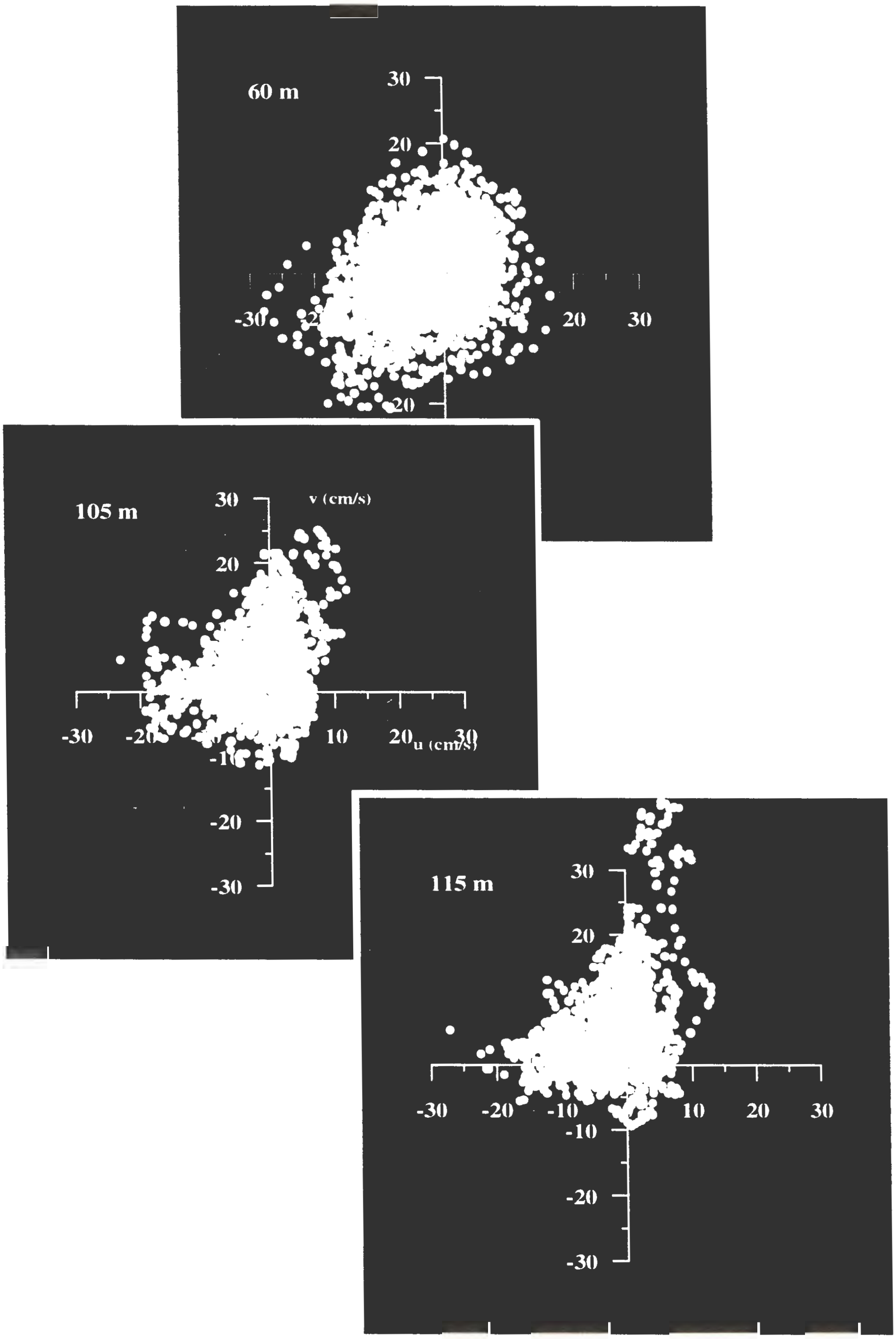

Appendix C12. u-components vs v-components from the station F9 during the second period.

Appendix C13

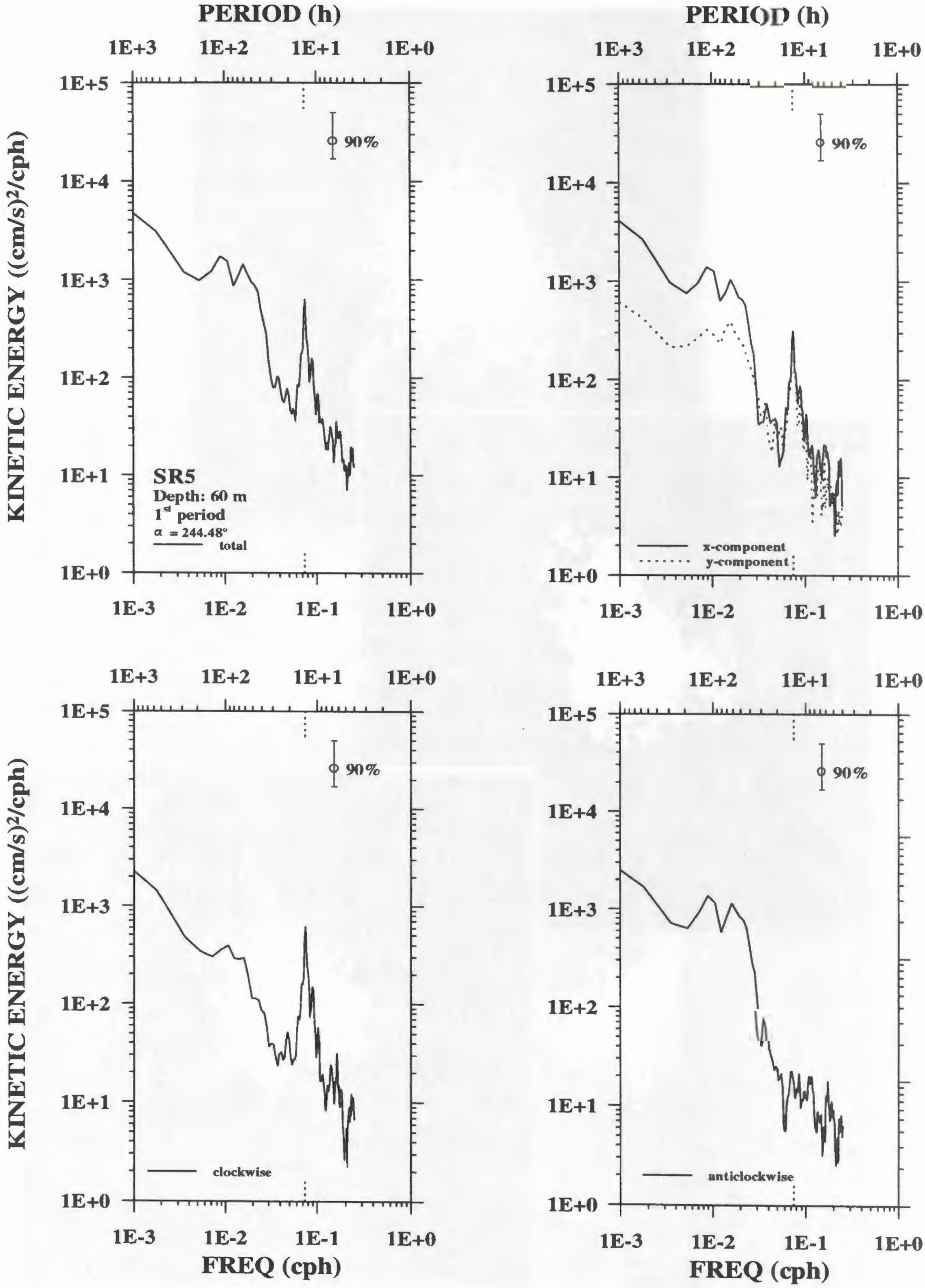

Appendix C13a. Energy spectra from station SR5, 60 m depth during the first period.

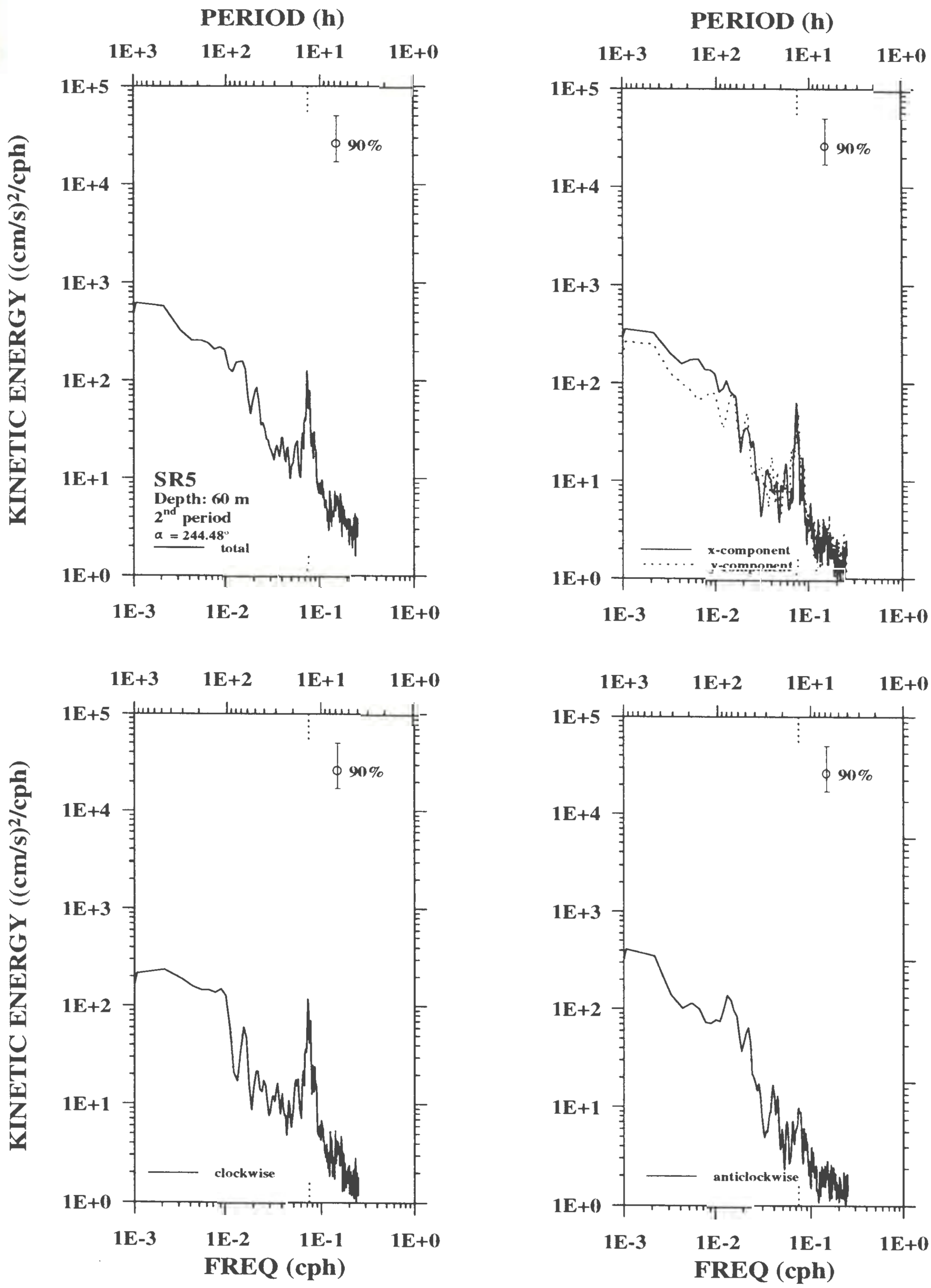

Appendix C13b. Energy spectra from station SR5, 60 m depth during the second period.

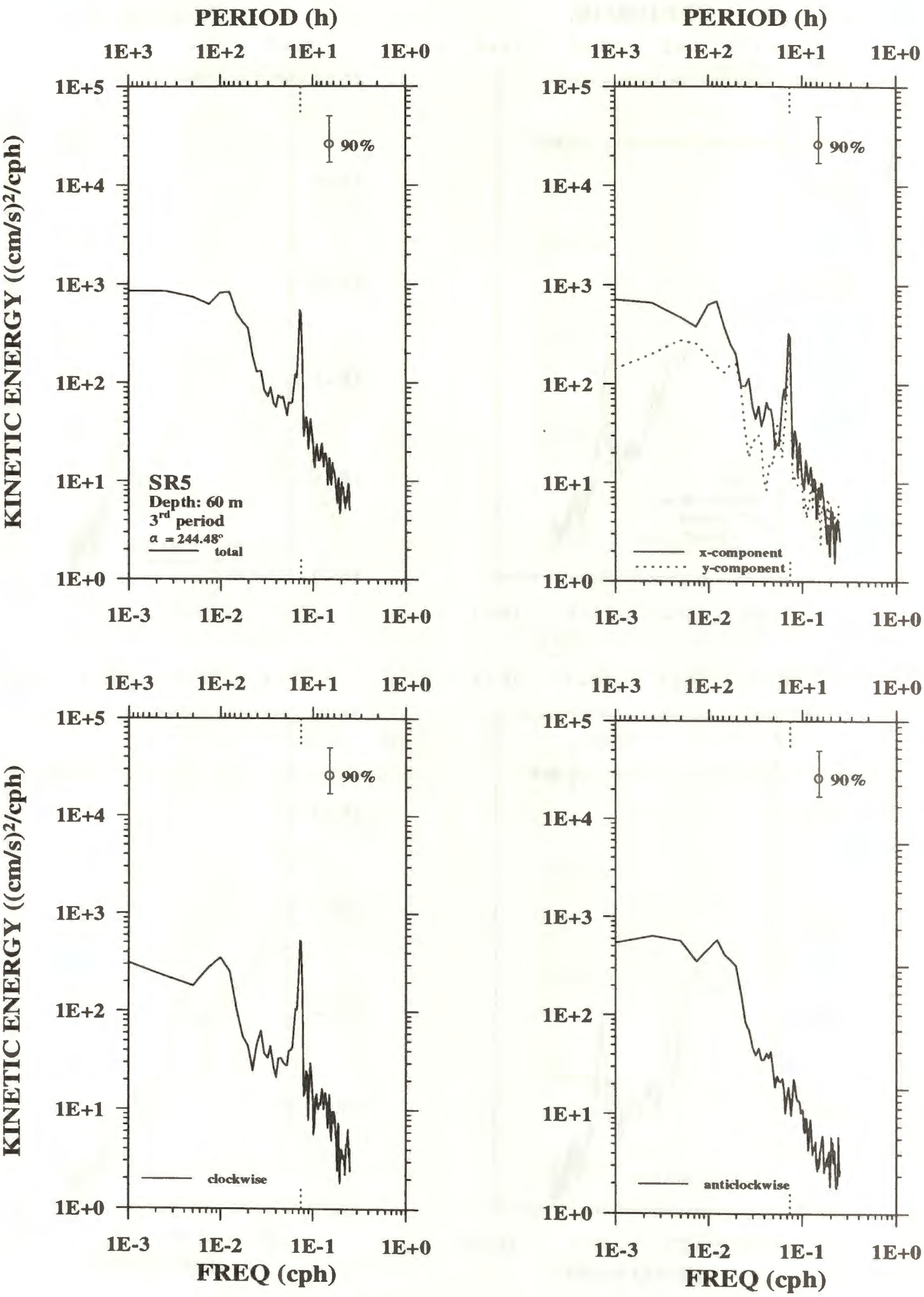

Appendix C13c. Energy spectra from station SR5, 60 m depth during the third period.

Appendix C14

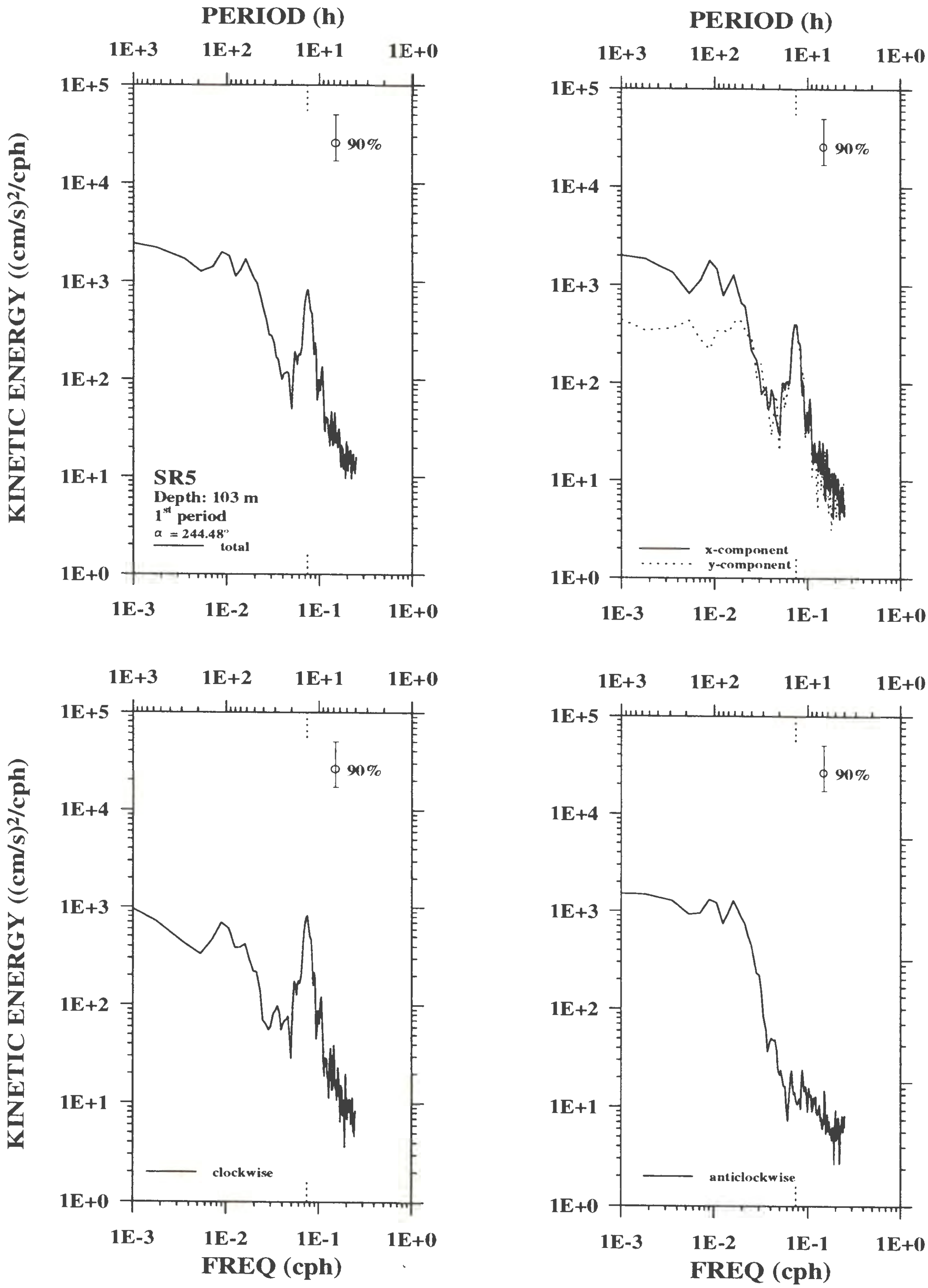

Appendix C14a. Energy spectra from station SR5, 103 m depth during the first period.

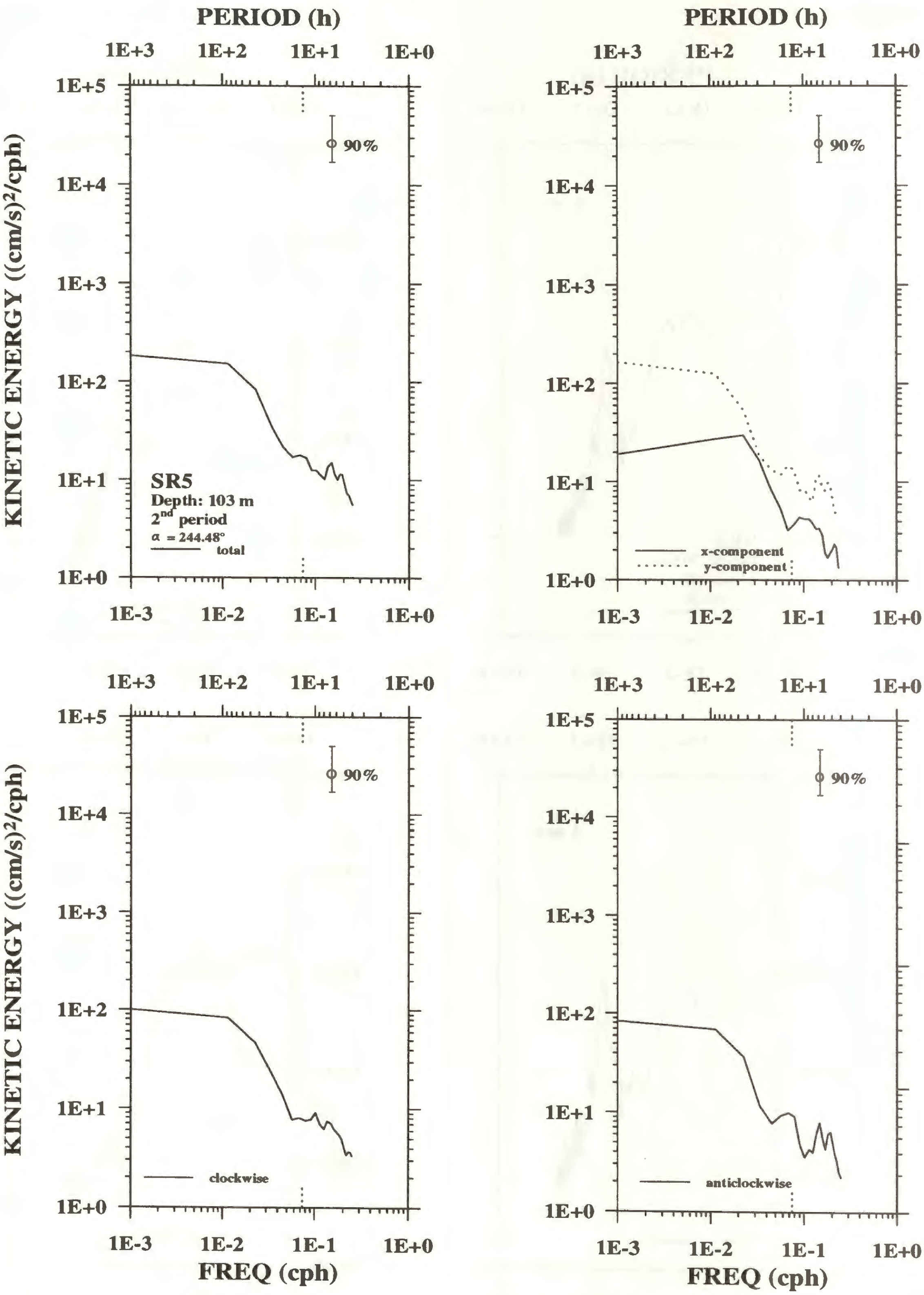

Appendix C14b. Energy spectra from station SR5, 103 m depth during the second period.

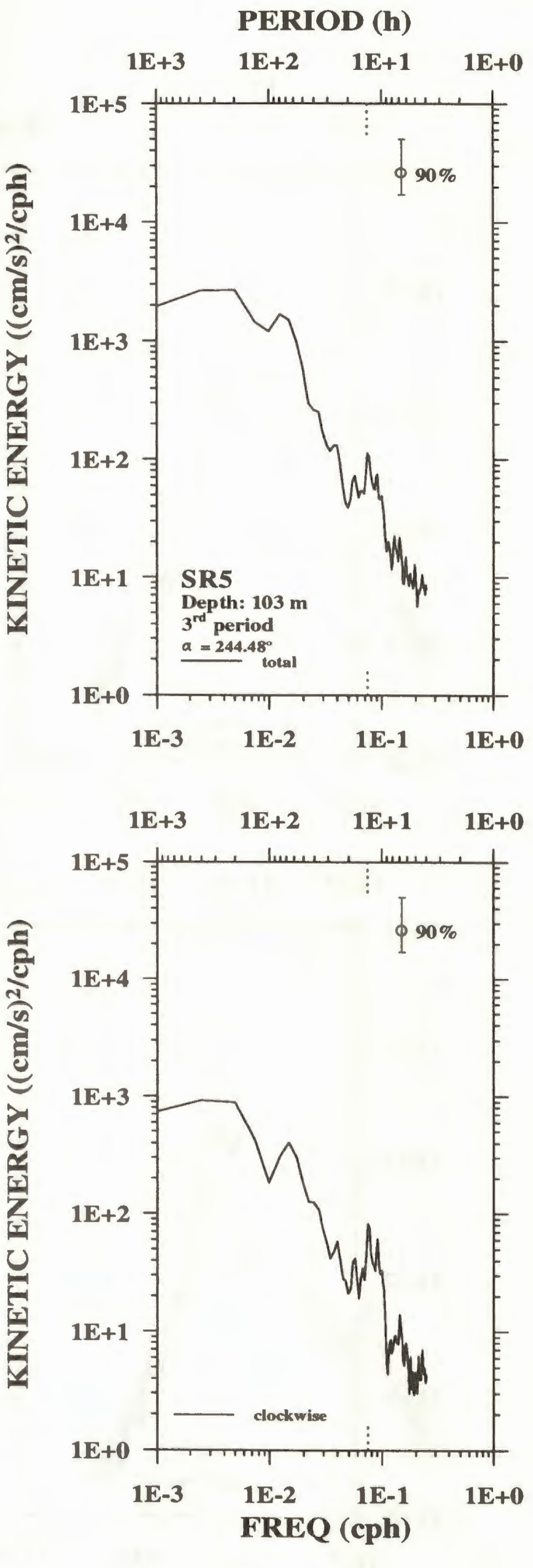

Appendix C14c. Energy spectra from station SR5, 103 m depth during the third period.

Appendix C15

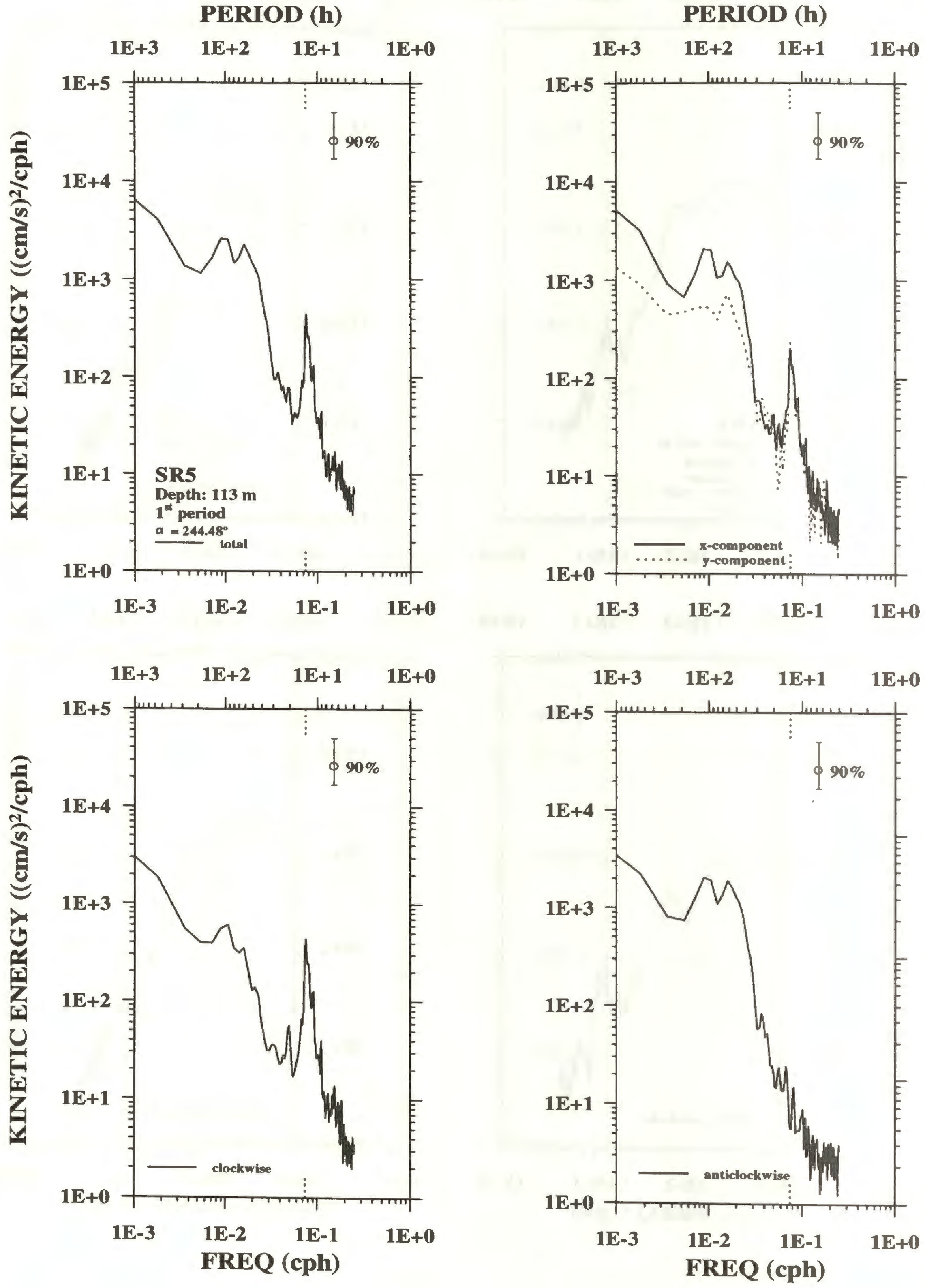

Appendix C15a. Energy spectra from station SR5, 113 m depth during the first period.

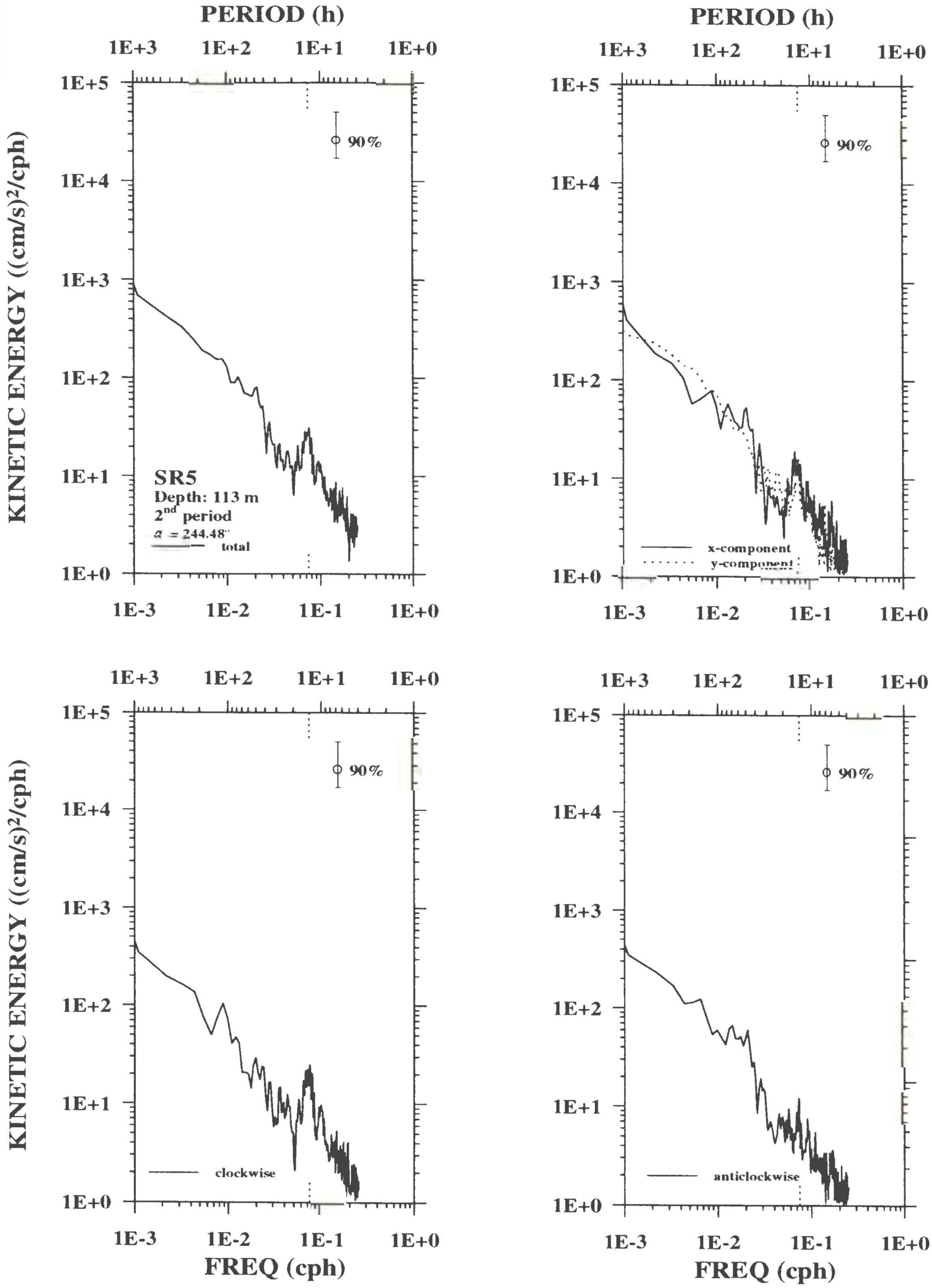

Appendix C15b. Energy spectra from station SR5, 113 m depth during the second period.

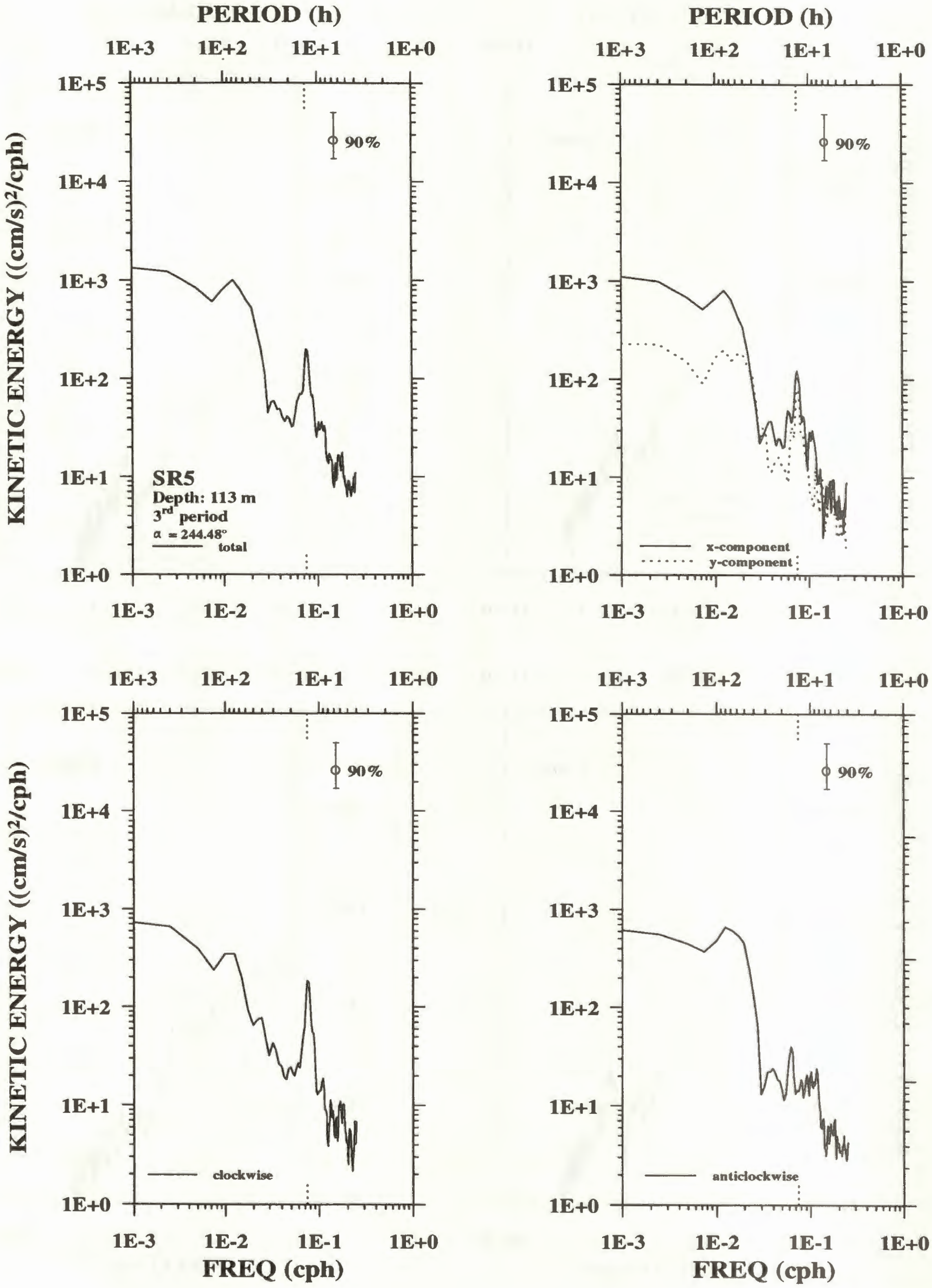

Appendix C15c. Energy spectra from station SR5, 113 m depth during the third period.

Appendix C16

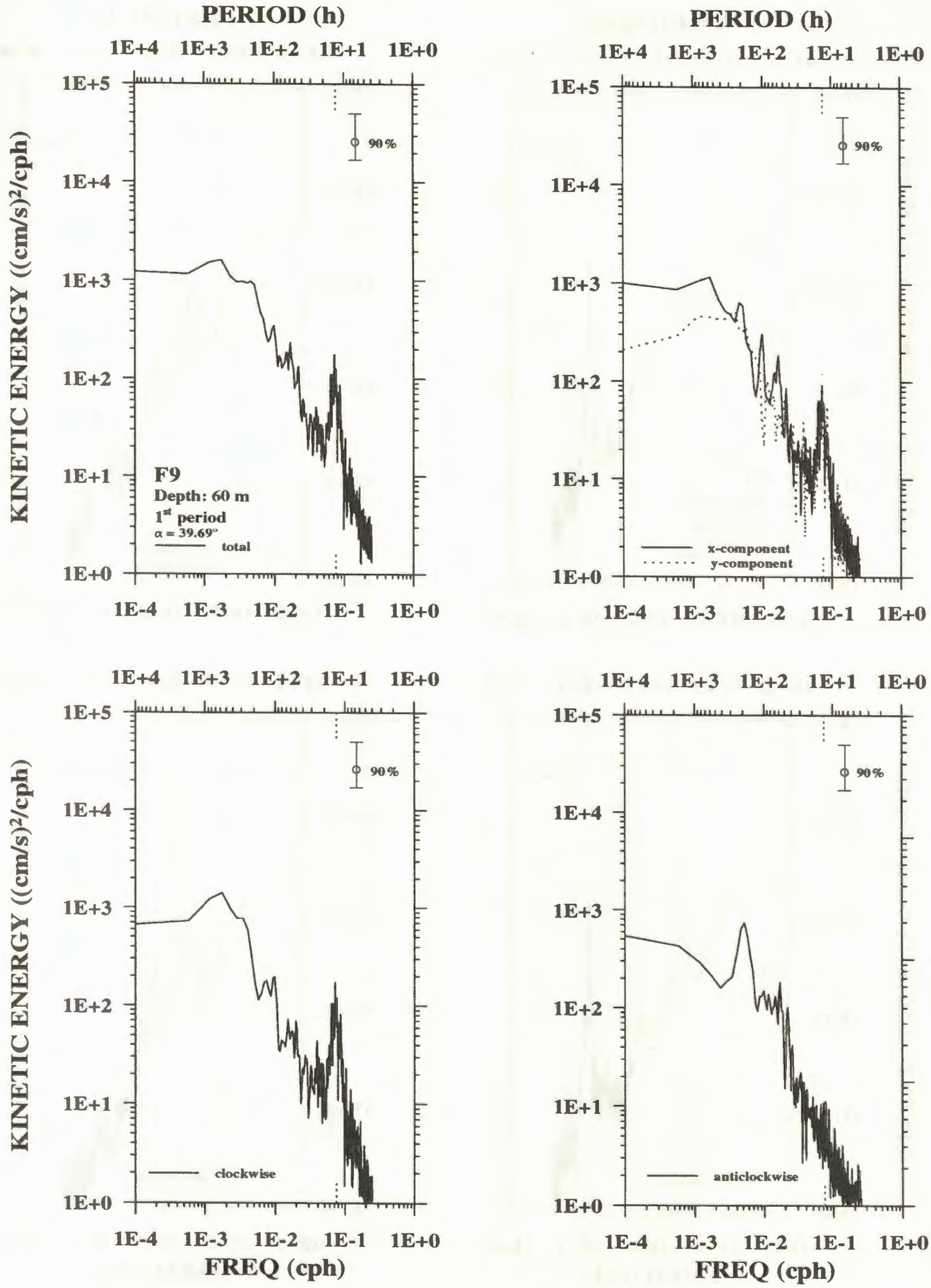

Appendix C16a. Energy spectra from station F9, 60 m depth during the first period.

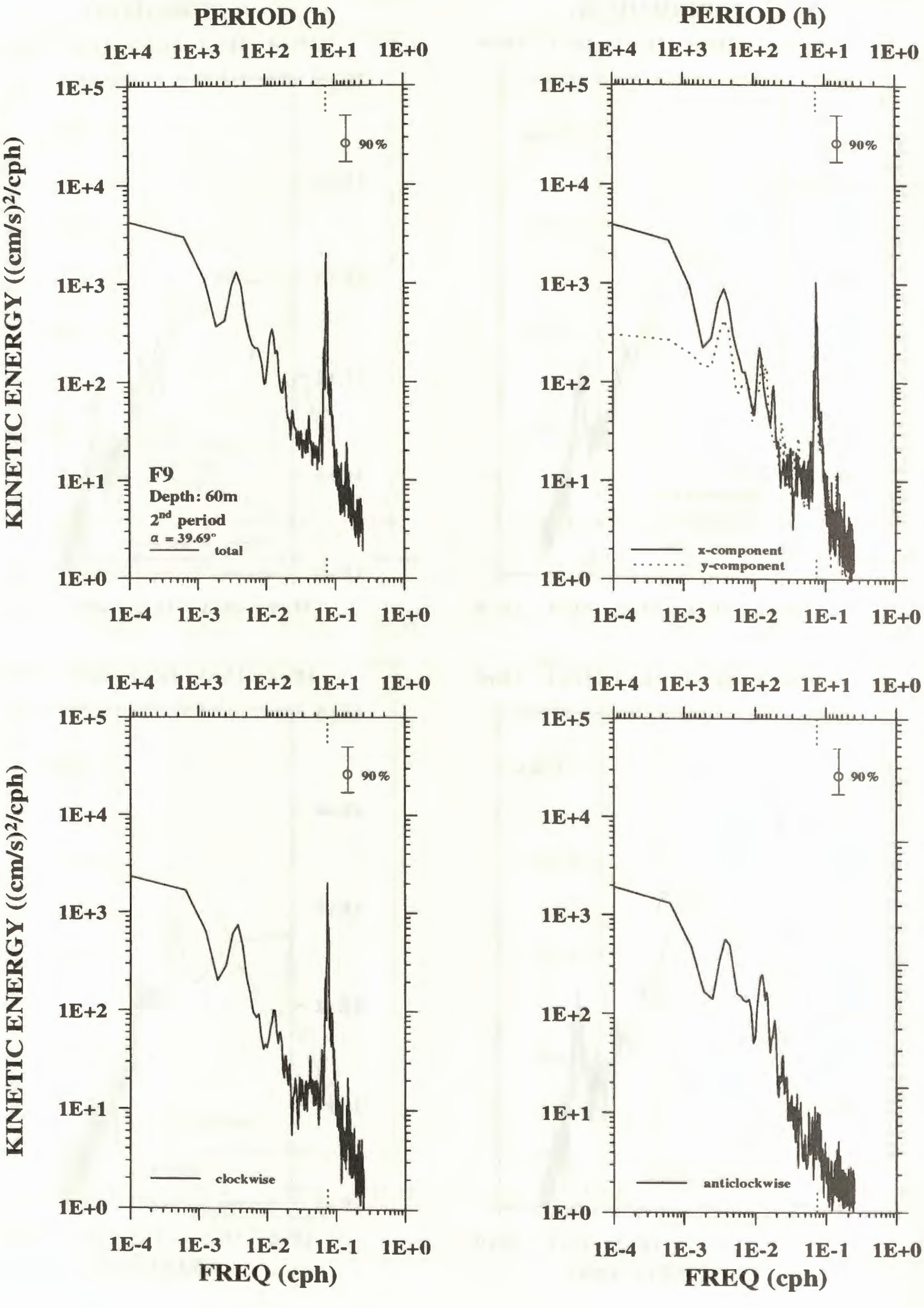

Appendix C16b. Energy spectra from station F9, 60 m depth during the second period.

Appendix C17

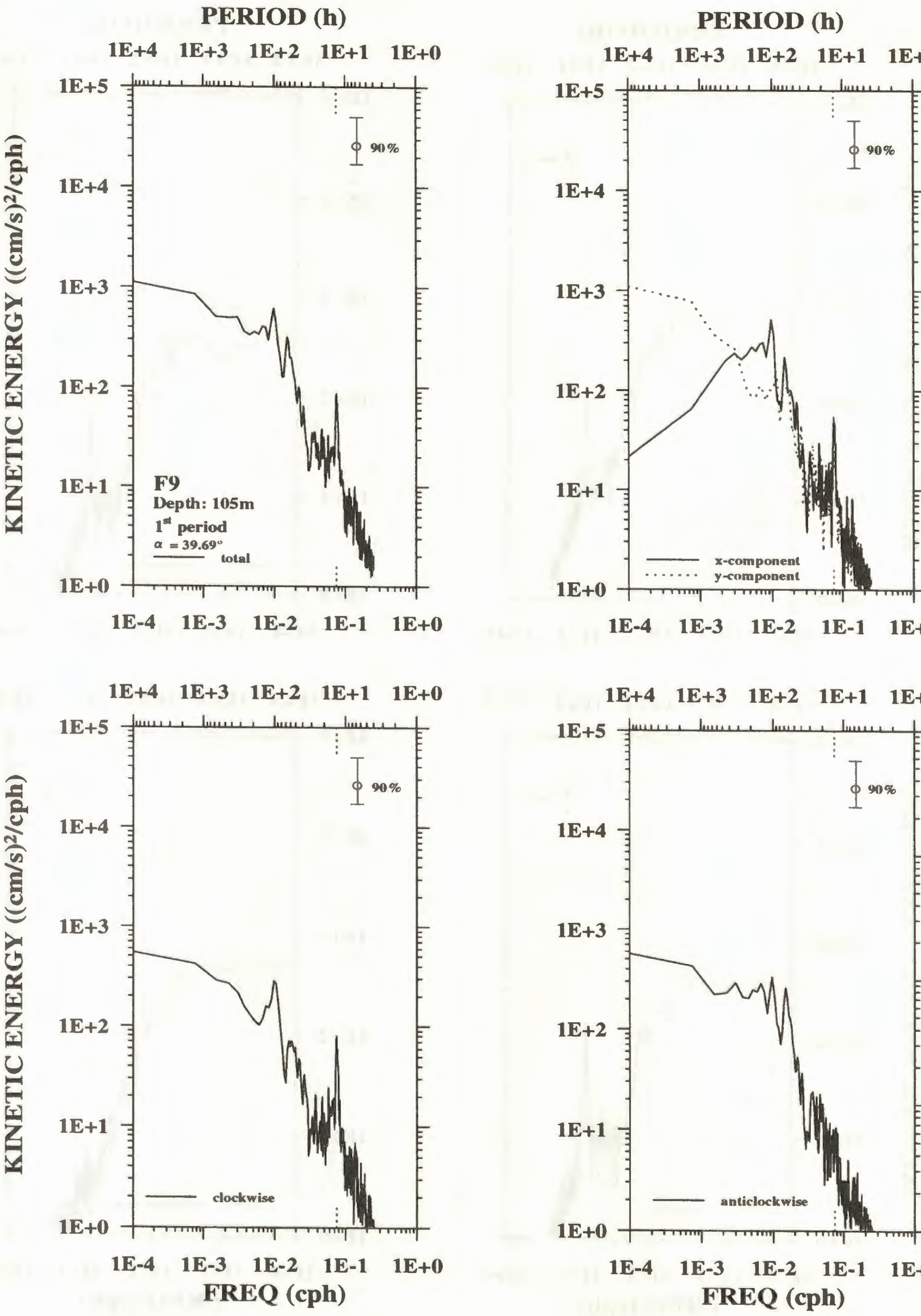

Appendix C17a. Energy spectra from station F9, 110 m depth during the first period.

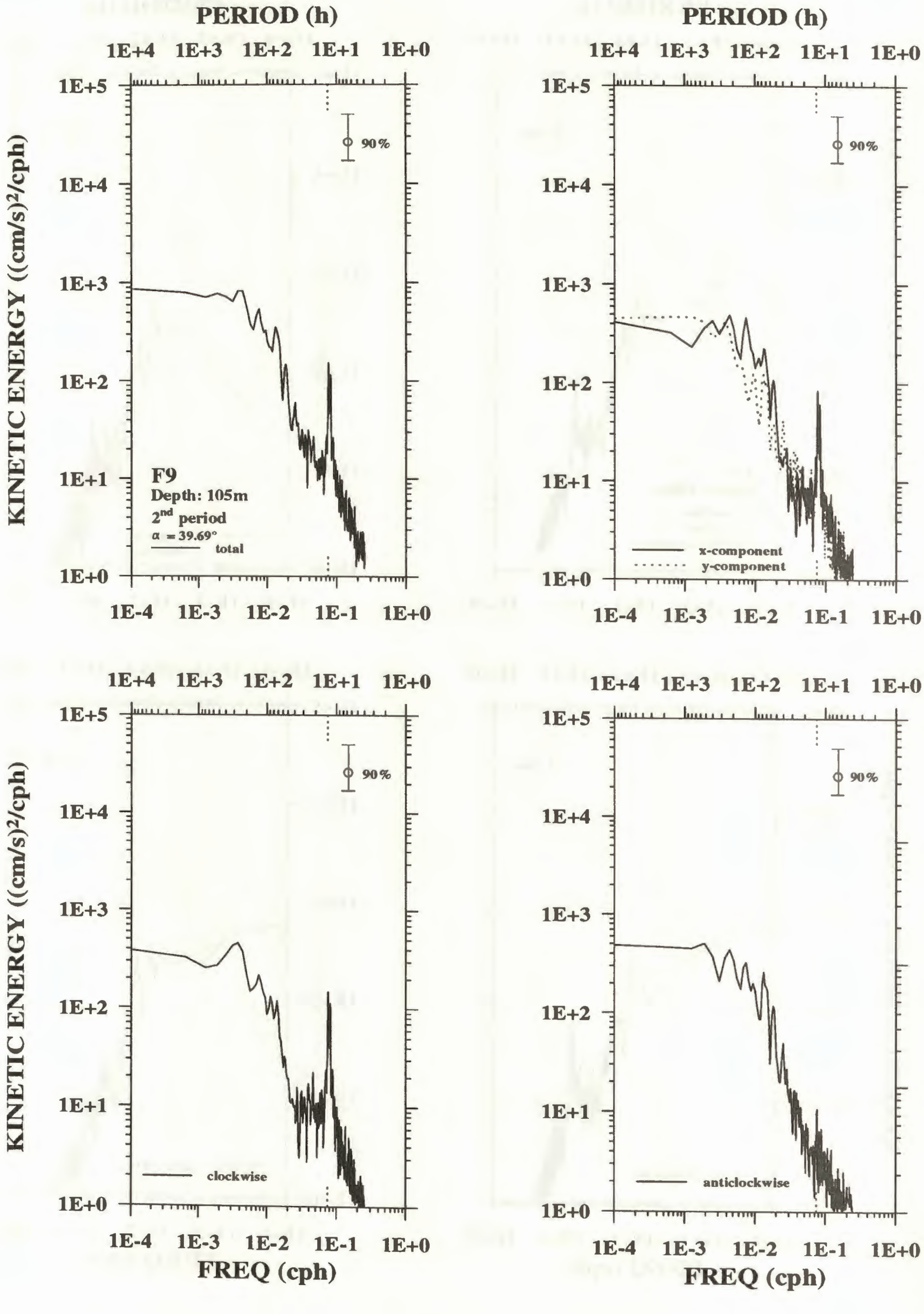

Appendix C17b. Energy spectra from station F9, 110 m depth during the second period.

Appendix C18

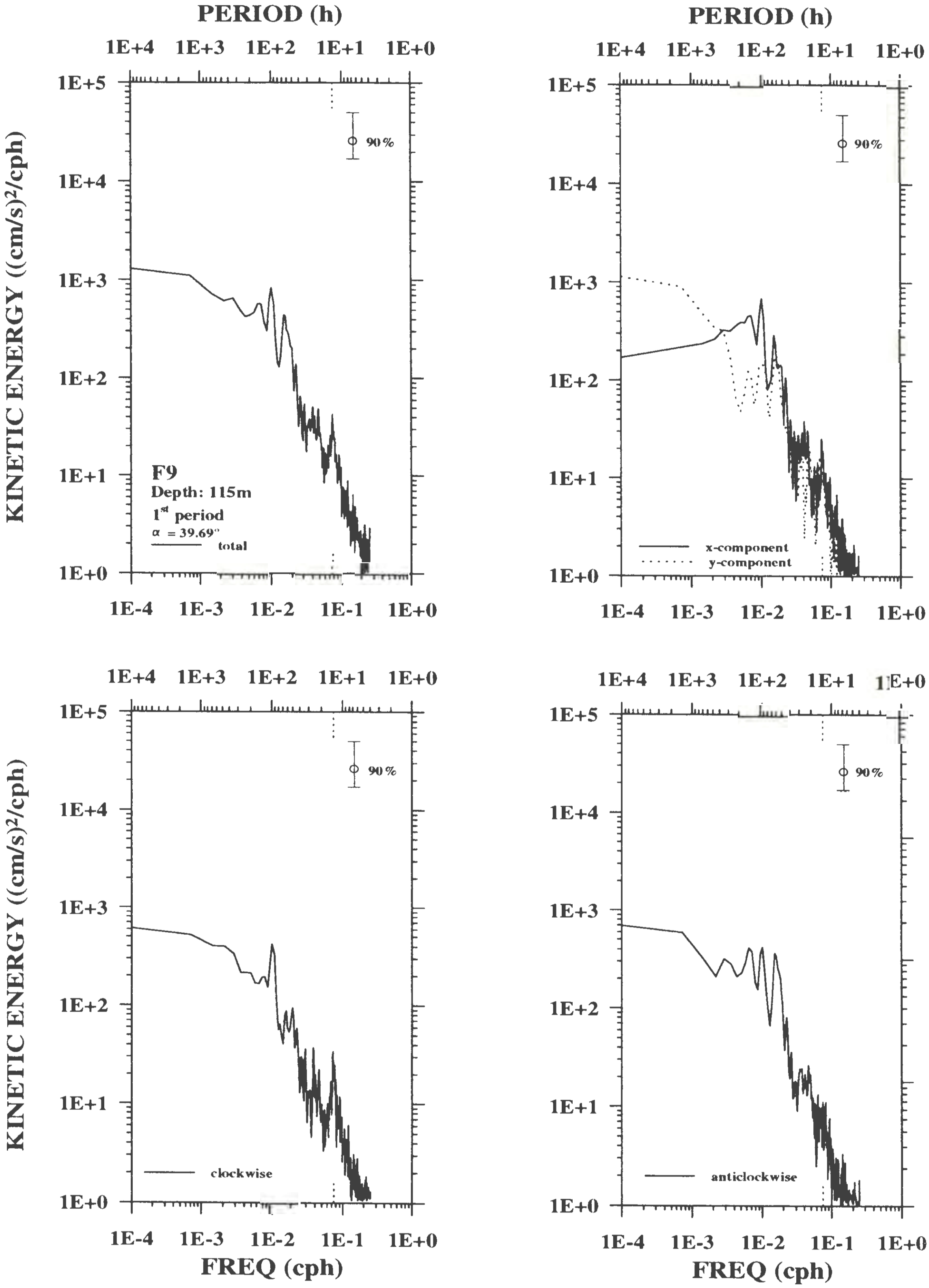

Appendix C18a. Energy spectra from station F9, 120 m depth during the first period.

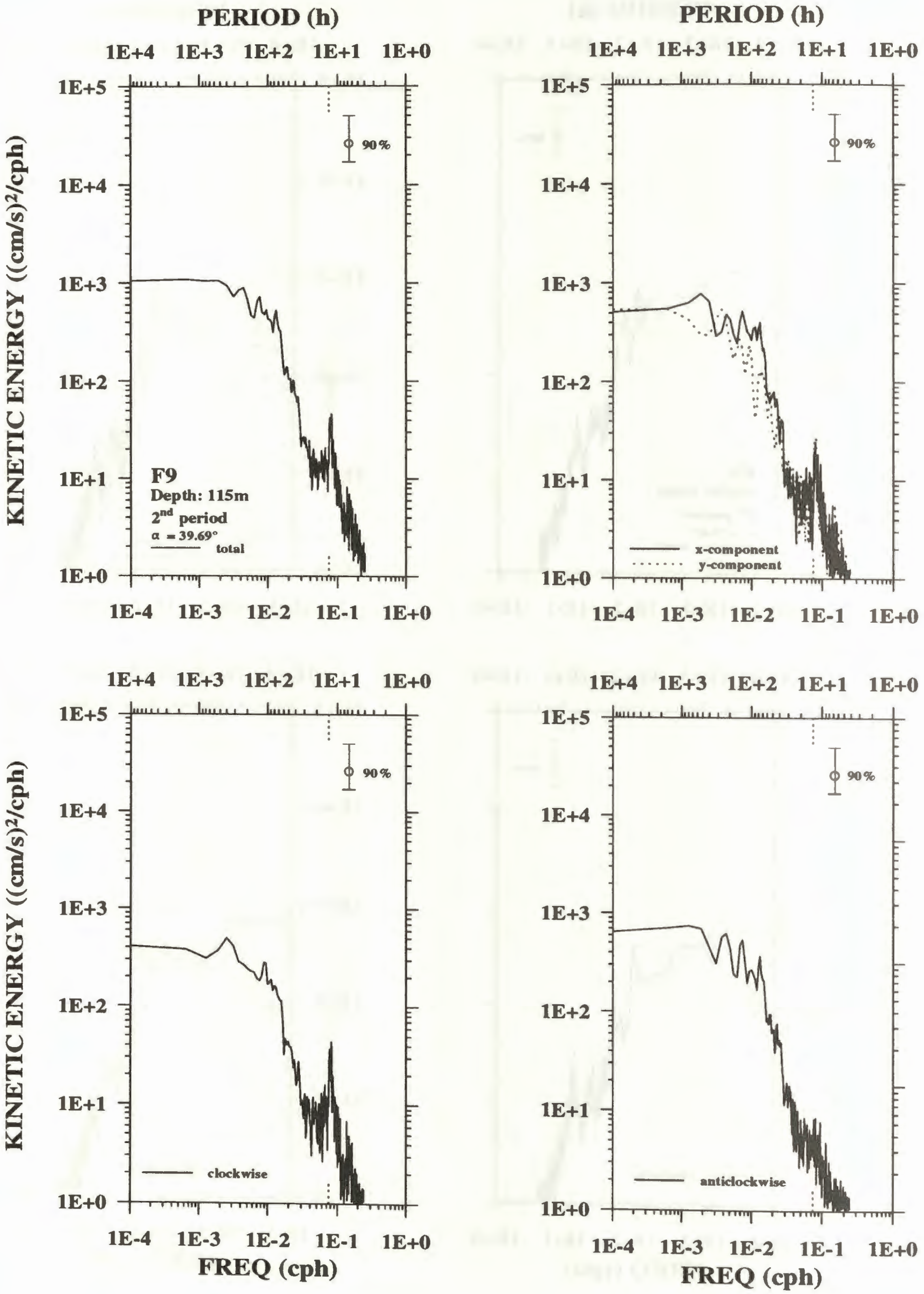

Appendix C18b. Energy spectra from station F9, 120 m depth during the second period.

Appendix C19

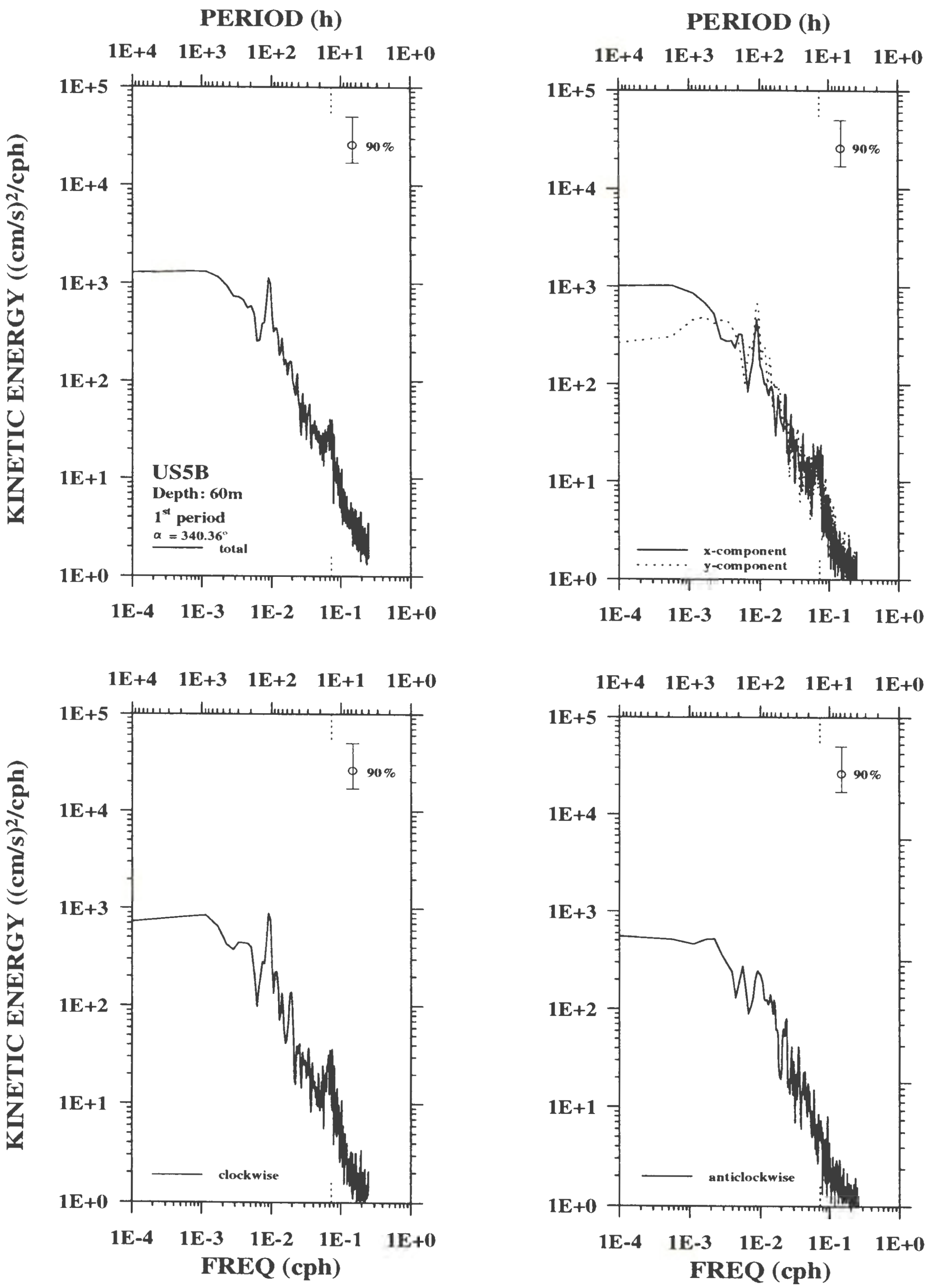

Appendix C19a. Energy spectra from station US5B, 60 m depth during the first period.

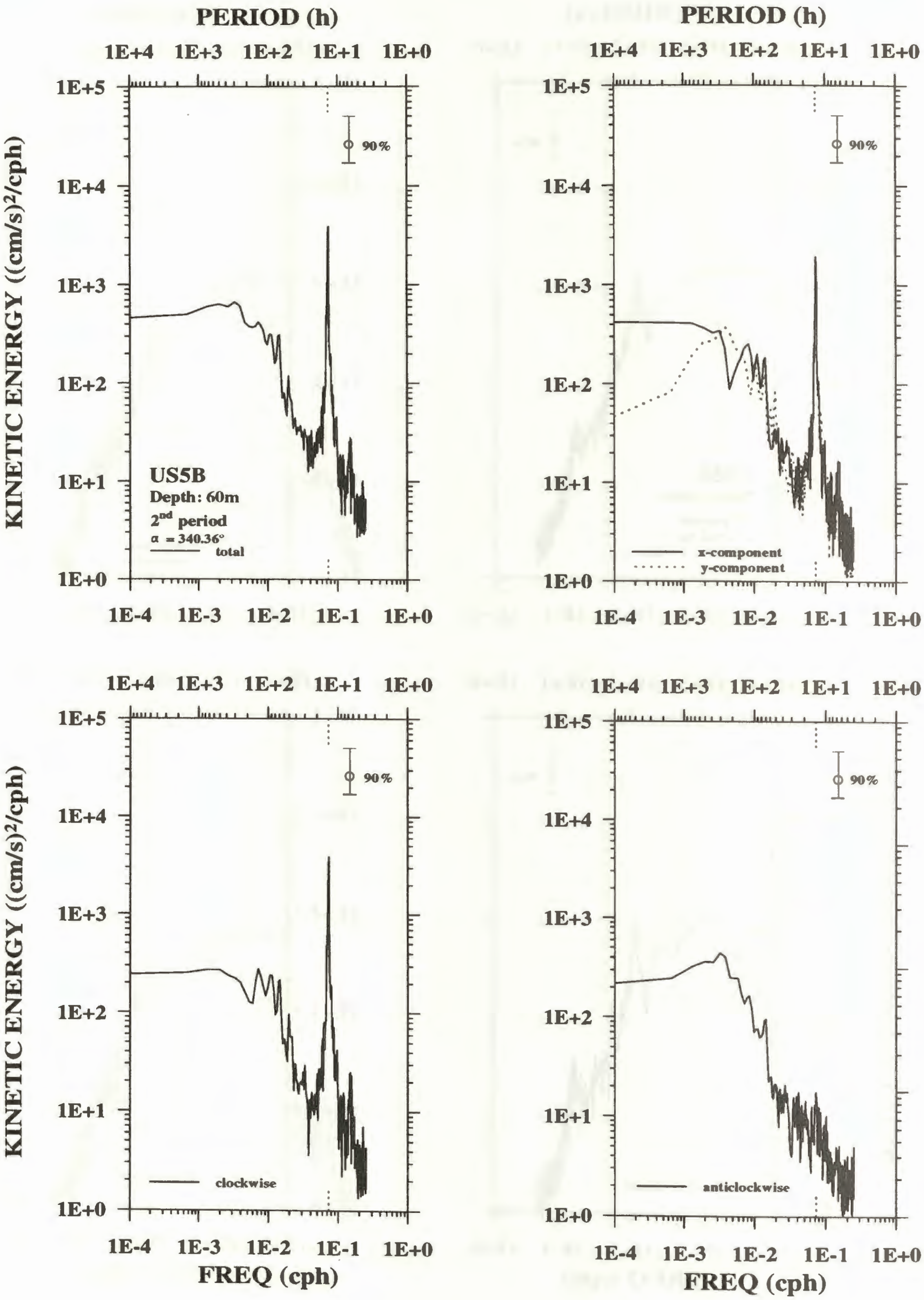

Appendix C19b. Energy spectra from station US5B, 60 m depth during the second period.

Appendix C20

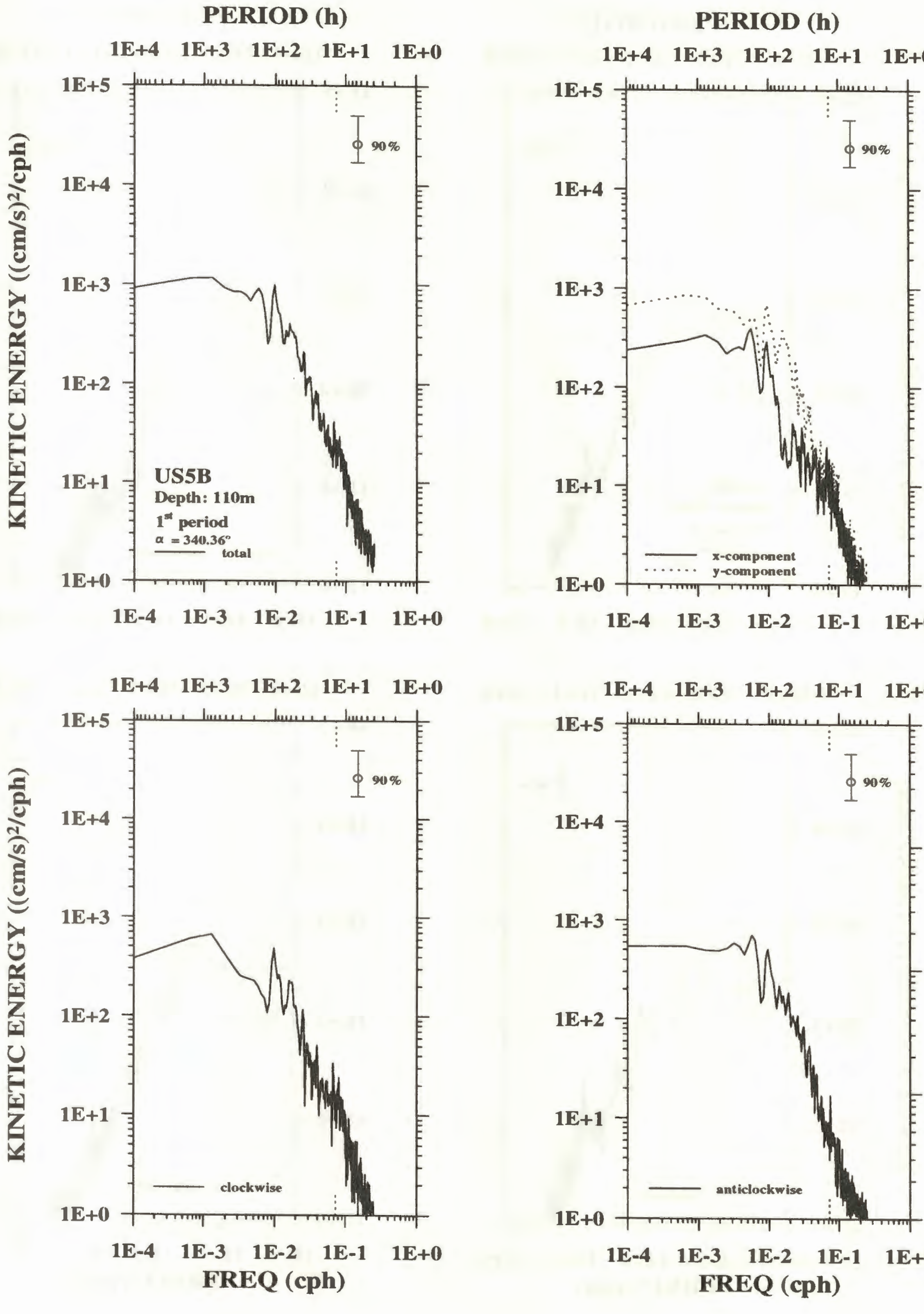

Appendix C20a. Energy spectra from station US5B, 110 m depth during the first period.

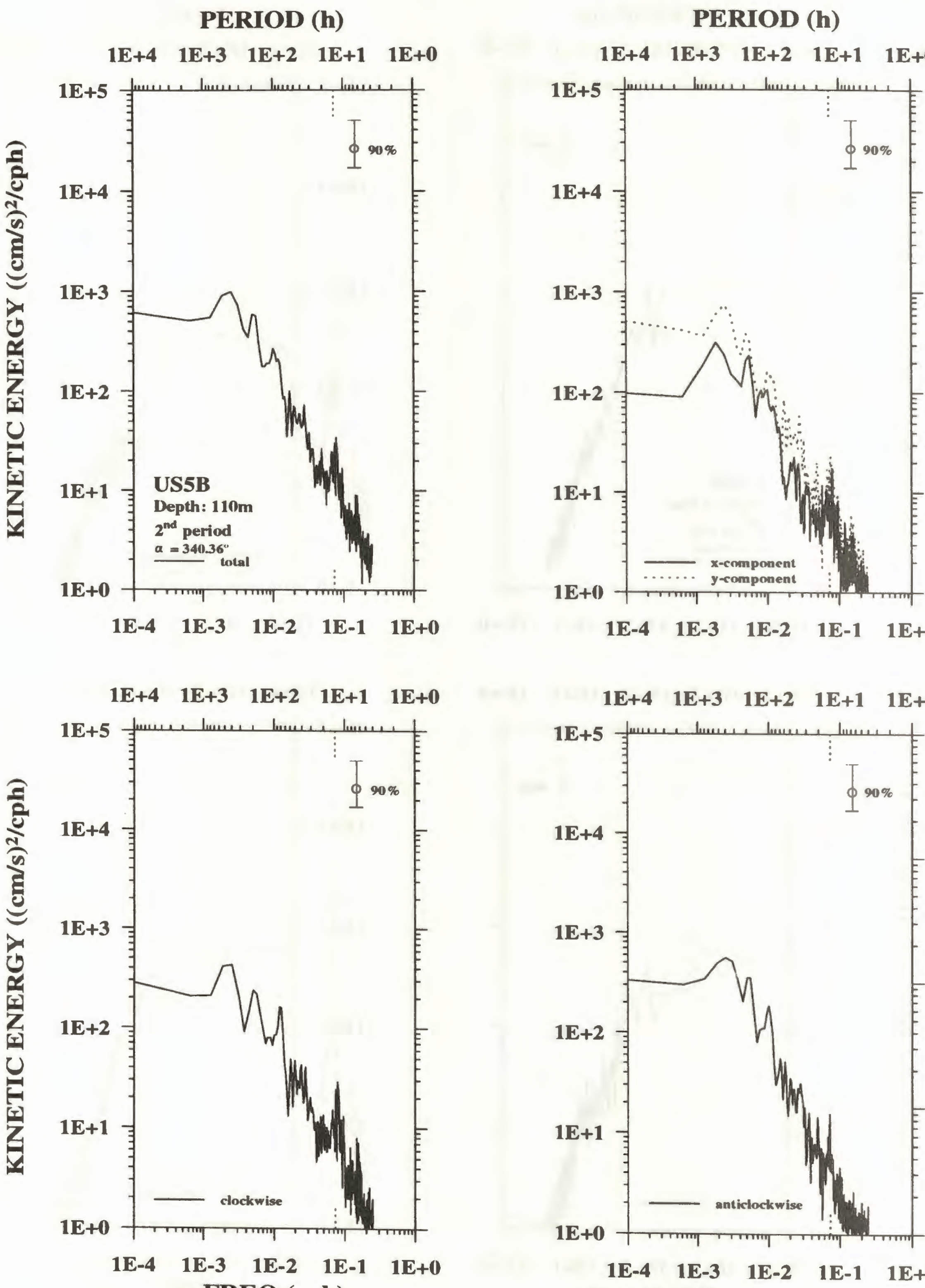

Appendix C20b. Energy spectra from station US5B, 110 m depth during the second period.

Appendix C21

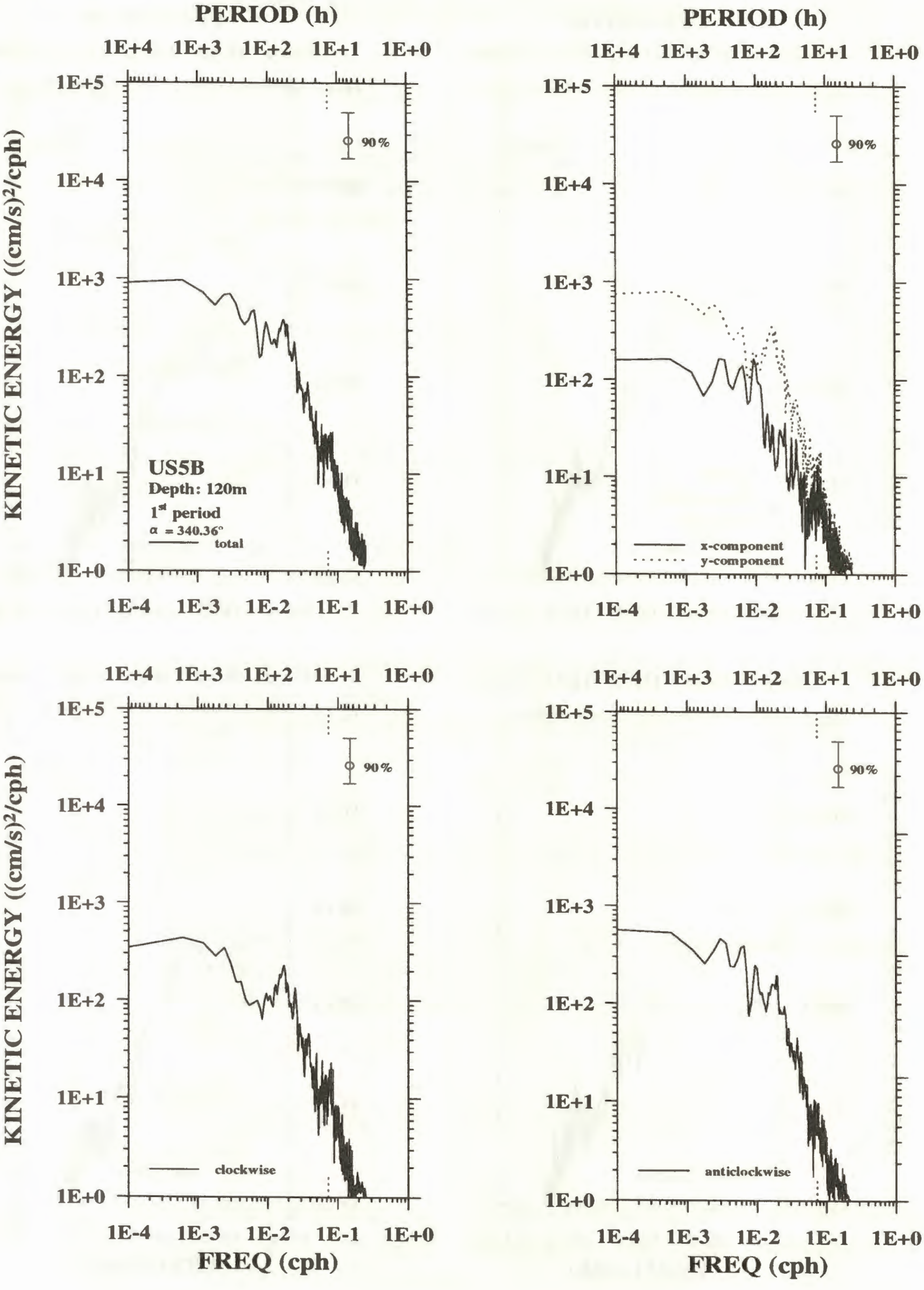

Appendix C21a. Energy spectra from station US5B, 120 m depth during the first period.

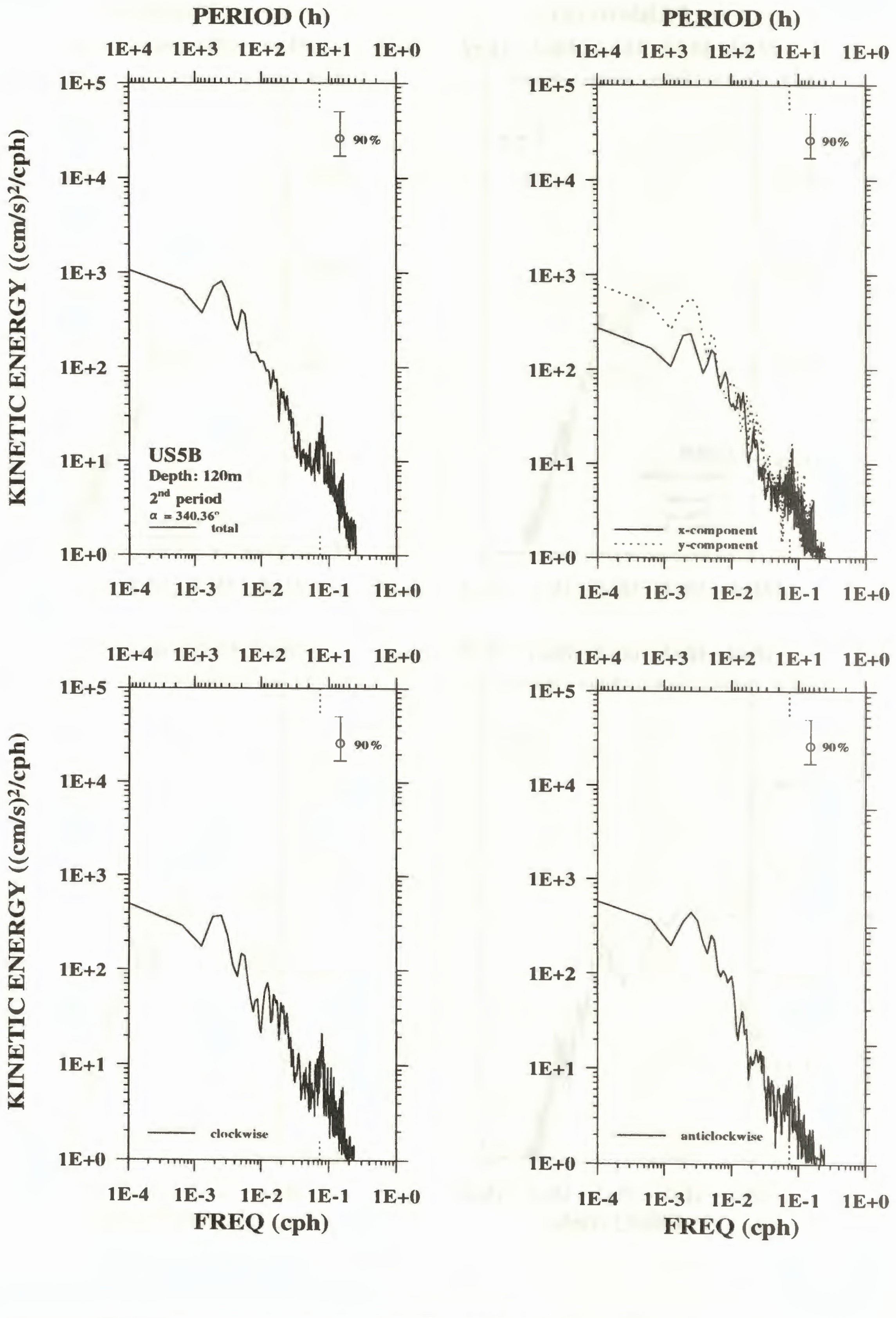

Appendix C21b. Energy spectra from station US5B, 120 m depth during the second period.

SMHI rapporter OCEANOGRAFI (RO)

Nr Titel

1 Lars Gidhagen, Lennart Funkquist and Ray Murthy.
Calculations of horizontal exchange coefficients using Eulerian time series current meter data from the Baltic Sea.
Norrköping 1986.

2 Thomas Thompson.
Ymer-80, satellites, arctic sea ice and weather.
Norrköping 1986.

3 Stig Carlberg et al.
Program för miljökvalitetsövervakning - PMK.
Norrköping 1986.

4 Jan-Erik Lundqvist och Anders Omstedt.
Isförhållandena i Sveriges södra och västra farvatten.
Norrköping 1987.

5 Stig Carlberg, Sven Engström, Stig Fonselius, Håkan Palmén, Eva-Gun Thelén, Lotta Fyrberg och Bengt Yhlen.
Program för miljökvalitetsövervakning - PMK. Utsjöprogram under 1986.
Göteborg 1987.

6 Jorge C. Valderama.
Results of a five year survey of the distribution of UREA in the Baltic sea.
Göteborg 1987.

7 Stig Carlberg, Sven Engström, Stig Fonselius, Håkan Palmén, Eva-Gun Thelén, Lotta Fyrberg, Bengt Yhlen och Danuta Zagradkin.
Program för miljökvalitetsövervakning - PMK. Utsjöprogram under 1987.
Göteborg 1988.

8 Bertil Håkansson.
Ice reconnaissance and forecasts in Storfjorden, Svalbard.
Norrköping 1988.

9 Stig Carlberg, Sven Engström, Stig Fonselius, Håkan Palmén, Eva-Gun Thelén, Lotta Fyrberg, Bengt Yhlen, Danuta Zagradkin, Bo Juhlin och Jan Szaron.
Program för miljökvalitetsövervakning - PMK. Utsjöprogram under 1988.
Göteborg 1989.

10 L. Fransson, B. Håkansson, A. Omstedt och L. Stehn.
Sea ice properties studied from the icebreaker Tor during BEPERS-88.
Norrköping 1989.

Nr Titel

11 Stig Carlberg, Sven Engström, Stig Fonselius, Håkan Palmén, Lotta Fyrberg, Bengt Yhlen, Bo Juhlin och Jan Szaron.
Program för miljökvalitetsövervakning - PMK. Utsjöprogram under 1989.
Göteborg 1990.

12 Anders Omstedt.
Real-time modelling and forecasting of temperatures in the Baltic Sea.
Norrköping 1990.

13 Lars Andersson, Stig Carlberg, Elisabet Fogelqvist, Stig Fonselius, Håkan Palmén, Eva-Gun Thelén, Lotta Fyrberg, Bengt Yhlen och Danuta Zagradkin.
Program för miljökvalitetsövervakning - PMK. Utsjöprogram under 1990.
Göteborg 1991.

14 Lars Andersson, Stig Carlberg, Lars Edler, Elisabet Fogelqvist, Stig Fonselius, Lotta Fyrberg, Marie Larsson, Håkan Palmén, Björn Sjöberg, Danuta Zagradkin, och Bengt Yhlen.
Haven runt Sverige 1991. Rapport från SMHI, Oceanografiska Laboratoriet, inklusive PMK - utsjöprogrammet.
(The conditions of the seas around Sweden. Report from the activities in 1991, including PMK - The National Swedish Programme for Monitoring of Environmental Quality Open Sea Programme.)
Göteborg 1992.

15 Ray Murthy, Bertil Håkansson and Pekka Alenius (ed.).
The Gulf of Bothnia Year-1991 - Physical transport experiments.
Norrköping 1993.

16 Lars Andersson, Lars Edler and Björn Sjöberg
The conditions of the seas around Sweden. Report from activities in 1992.
Göteborg 1993.

17 Anders Omstedt, Leif Nyberg and Matti Leppäranta.
A coupled ice-ocean model supporting winter navigation in the Baltic Sea.
Part 1. Ice dynamics and water levels.
Norrköping 1994.

18 Lennart Funkquist.
An operational Baltic Sea circulation model. Part 1. Barotropic version.
Norrköping 1993.

19 Marmefelt, Eleonor.
Currents in the Gulf of Bothnia. During the Field Year of 1991.
Norrköping 1994.

SMHI

Swedish Meteorological and Hydrological Institute
S-601 76 Norrköping, Sweden. Tel. +4611158000. Telex 644 00 smhi s.